

Spring 2022

Steric Effect on Benzyl Ether Olefines Under SADMET Polymerization

Su Hu
San Jose State University

Follow this and additional works at: https://scholarworks.sjsu.edu/etd_theses

Recommended Citation

Hu, Su, "Steric Effect on Benzyl Ether Olefines Under SADMET Polymerization" (2022). *Master's Theses*. 5266.

DOI: <https://doi.org/10.31979/etd.q2uz-sxmh>
https://scholarworks.sjsu.edu/etd_theses/5266

This Thesis is brought to you for free and open access by the Master's Theses and Graduate Research at SJSU ScholarWorks. It has been accepted for inclusion in Master's Theses by an authorized administrator of SJSU ScholarWorks. For more information, please contact scholarworks@sjsu.edu.

STERIC EFFECT ON BENZYL ETHER OLEFINS UNDER SADMET
POLYMERIZATION

A Thesis

Presented to

The Faculty of the Department of Chemistry

San José State University

In Partial Fulfillment

of the Requirements for the Degree

Master of Chemistry

by

Su Hu

April 2022

© 2022

Steric Effect On Benzyl Ether Olefins Under Sadmet Polymerization

ALL RIGHTS RESERVED

The Designated Thesis Committee Approves the Thesis Titled

STERIC EFFECT ON BENZYL ETHER OLEFINS UNDER SADMET
POLYMERIZATION

by

Su Hu

APPROVED FOR THE DEPARTMENT OF CHEMISTRY

SAN JOSÉ STATE UNIVERSITY

April 2022

Chester Simocko, Ph.D.	Department of Chemistry
Madalyn Radlauer, Ph.D.	Department of Chemistry
Philip Dirlam, Ph.D.	Department of Chemistry
Roger Terrill, PhD.	Department of Chemistry

ABSTRACT

STERIC EFFECT ON BENZYL ETHER OLEFINS UNDER SADMET POLYMERIZATION

by Su Hu

Acyclic diene metathesis (ADMET) polymerization, a type of olefin cross metathesis, is a step-growth and condensation polymerization that can be used to synthesize hydrocarbon polymers with diverse functional groups. Traditional ADMET with symmetric α,ω -dienes is not selective and can only form homopolymers or statistical copolymers. Changing to monomers with acrylate functional groups allows selective reactivity to form block and alternating polymers. In this project, we want to explore other functional groups that result in selective reactivity to form advanced polymer architectures via what we have termed selective acyclic diene metathesis (SADMET) polymerization. Developing new functionalized monomers for SADMET polymerization allows for the synthesis of precision alternating copolymers with a variety of backbone chemistries, pendant groups, and tacticity. In addition, the steric effect around the monomers double bonds was examined with the goal of finding more monomers that can be used to make block or alternating polymers via SADMET polymerization. With this control over the polymer chain, the newly engineered polymers could be applied to ion transport, drug delivery, and polymer self-assembly

ACKNOWLEDGEMENTS

I could not finish this research and thesis without the help and support from people around me during the pandemic period. Firstly, I would like to thank those groupmates I met. Especially, Ryan Nhan and Matt Dahlberg, we started doing research together from undergraduate, and they gave me many suggestions when I had troubles. Thanks to Yan and Leo for staying with me during the demanding time in university and for constant encouragement after leaving. My previous research tutors, Hasaan Shariq Rauf and Jasleen Sahota, trained and helped me understand the research that was relatively new to me at first.

Also, I sincerely acknowledge all my committee members. Dr. Dirlam and Dr. Terrill provided advice for improvements in the process. As my second research advisor, Dr. Radlauer helped me as much as possible, both in the experiment and life. Her insightful feedback pushed me to sharpen my thinking through each stage of process. With many thanks to my PI, Dr. Simocko, for his valuable guidance throughout my studies and research and for giving me opportunities to learn and present at academic conferences. Thank you both research advisors, for always being there to help me when I needed it.

Finally, I want to thank my family and friends for their company and support outside of the research. They provided stimulating discussions as well as happy distractions to rest my mind.

TABLE OF CONTENTS

List of Tables	viii
List of Figures	ix
1 Introduction.....	1
1.1 Olefin Metathesis	1
1.2 Chauvin Mechanism	2
1.3 Catalyst Development.....	3
1.3.1 Schrock Catalyst	4
1.3.2 Grubbs Catalyst.....	5
1.4 ADMET Polymerization.....	6
1.4.1 ADMET Polymerization Conditions	7
1.4.2 Applications	7
1.4.3 Drawbacks.....	8
1.5 SADMET Polymerization.....	8
1.5.1 Olefins Categorizations.....	9
1.5.2 Research Goal	10
2 Synthesis of Monomers.....	12
2.1 Background	12
2.2 Material and Methods	13
2.2.1 General Information.....	13
2.2.2 Representative Procedure.....	13
2.3 Result	15
2.3.1 M1 (1,4-Bis[(2-propen-1-yloxy)methyl]benzene).....	15
2.3.2 M2 (1,4-Bis[[1-methyl-2-propen-1-yl]oxy]methyl]benzene)	16
2.3.3 M3 (1,4-Bis[[3-methyl-3-buten-1-yl]oxy]methyl]benzene).....	18
2.3.4 M4 (1,4-Bis[[1,1-dimethyl-2-propen-1-yl]oxy]methyl]benzene)	19
2.4 Discussion	21

3	Homopolymerizations.....	22
	3.1 Background.....	22
	3.2 Material and Methods.....	23
	3.2.1 General Information.....	23
	3.2.2 Representative Procedures.....	23
	3.3 Results.....	25
	3.3.1 Homopolymerizations of M1.....	25
	3.3.2 Homopolymerizations of M2.....	26
	3.3.3 Homopolymerizations of M3.....	28
	3.3.4 Homopolymerizations of M4.....	30
	3.4 Discussion.....	32
4	Copolymerizations with 1,9-Decadiene.....	33
	4.1 Background.....	33
	4.2 Material & Methods.....	34
	4.2.1 General Information.....	34
	4.3 Result.....	34
	4.3.1 Copolymerization of M2.....	34
	4.3.2 Copolymerization of M3.....	36
	4.3.3 Copolymerization of M4.....	38
	4.4 Discussion.....	41
5	Conclusion and Future Work.....	43
	5.1 Conclusion.....	43
	5.1.1 Olefin Categorization.....	43
	5.1.2 Steric Effects.....	44
	5.2 Future Works.....	46
	References.....	47

LIST OF TABLES

Table 1. Categorization of olefins for SADMET polymerization.	10
Table 2. Four α , ω -diene monomers designed and synthesized for this project.	13
Table 3. Alcohol starting materials for monomers M1-M4.....	14
Table 4. Polymerization results and classifications of M1 – M4 with G1 and G2.	45

LIST OF FIGURES

Figure 1. Categories of olefin metathesis reactions. (a) Ring-closing metathesis (RCM), ring-opening metathesis polymerization (ROMP), acyclic diene metathesis (ADMET), and (b) cross-metathesis (CM). Figure reproduced from reference 9.	2
Figure 2. Chauvin mechanism of olefin metathesis.	3
Figure 3. Common homogeneous metathesis catalysts (a) The first reported Schrock catalyst, (b) First, and (c) second generation Grubbs catalysts.	5
Figure 4. Synthesis of alternating copolymers via a) primary ADMET polymerization and b) secondary SADMET polymerization.	9
Figure 5. General model for monomer synthesis.	13
Figure 6. ^1H NMR spectrum of M1.	15
Figure 7. ^{13}C NMR spectrum of M1.	16
Figure 8. ^1H NMR spectrum of M2.	17
Figure 9. ^{13}C NMR spectrum of M2.	17
Figure 10. ^1H NMR spectrum of M3.	18
Figure 11. ^{13}C NMR spectrum of M3.	19
Figure 12. ^1H NMR spectrum of M4.	20
Figure 13. ^{13}C NMR spectrum of M4.	20
Figure 14. General ADMET homopolymerization reaction conditions.	22
Figure 15. ^1H NMR spectrum of the homopolymerization of M1 with G2 as the catalyst.	26
Figure 16. ^1H NMR spectrum of the homopolymerization attempt of M2 with G1 as the catalyst.	27
Figure 17. ^1H NMR spectrum of the homopolymerization of M2 with G2 as the catalyst.	28
Figure 18. ^1H NMR spectrum of the homopolymerization attempt of M3 with G1 as the catalyst.	29

Figure 19. ^1H NMR spectrum of the homopolymerization attempt of M3 with G2 as the catalyst.	29
Figure 20. ^1H NMR spectrum of the homopolymerization attempt of M4 with G1 as the catalyst.	31
Figure 21. ^1H NMR spectrum of the homopolymerization attempt of M4 with G2 as the catalyst.	31
Figure 22. GPC analysis of homopolymer.....	32
Figure 23. General scheme for copolymerization with 1,9-decadiene under SADMET conditions.	33
Figure 24. ^1H NMR spectrum of the copolymerization of M2 with G1 as the catalyst.....	35
Figure 25. COSY NMR spectrum of the copolymerization of M2 with G1 as the catalyst.	36
Figure 26. ^1H NMR spectrum of the copolymerization of M3 with G1 as the catalyst.....	37
Figure 27. ^1H NMR spectrum of the copolymerization of M3 with G2 as the catalyst.....	38
Figure 28. COSY NMR spectrum of the copolymerization of M3 with G2 as the catalyst.	38
Figure 29. ^1H NMR spectrum of the copolymerization of M4 with G1 as the catalyst.....	40
Figure 30. ^1H NMR spectrum of the copolymerization of M4 with G2 as the catalyst.....	40
Figure 31. COSY NMR spectrum of the copolymerization of M4 with G2 as the catalyst.	41
Figure 32. GPC analysis of copolymers.	41

Introduction

1.1 Olefin Metathesis

Olefin metathesis (OM) is a rearrangement between carbon-carbon double bonds in which metal carbene complexes catalyze the redistribution.¹ Because of mild reaction conditions and conventional procedures with multiple efficient catalysts, OM has become a versatile tool from organometallic to organic and polymer chemistry.² Moreover, those conveniences present fewer additional reagents and byproducts than traditional methods, like Boord and Fischer–Tropsch olefin synthesis.³

The major developments in OM research have all taken place in the last 70 years. The first OM reaction was observed in the mid-1950s, bicyclo-(2,2,1)-2-heptene, with a reorganization of carbon-carbon double bonds.⁴ Catalyzed olefin metathesis was further explored by Ziegler research group.⁴⁻⁶ After this discovery of OM, there were many hypotheses about the mechanism, and the most prominent catalytical mechanism was the one proposed by Chauvin and co-workers in the 1970s.⁷ It emphasized the interactions between the olefinic substrates and the metal carbene complexes, which explains the catalyst role in OM reactions (see Section 1.2).⁷ It was not until the 1990s that two crucial catalyst systems were discovered: molybdenum-based Schrock catalysts and ruthenium-based Grubbs catalysts.⁸ Since then, many variations of the original Schrock and Grubbs catalysts have been developed, and the transformations they perform have been subdivided into several categories, including ring-closing metathesis (RCM), ring-opening metathesis polymerization (ROMP and ROM), cross-metathesis (CM), and acyclic diene metathesis (ADMET) (Figure 1).⁹

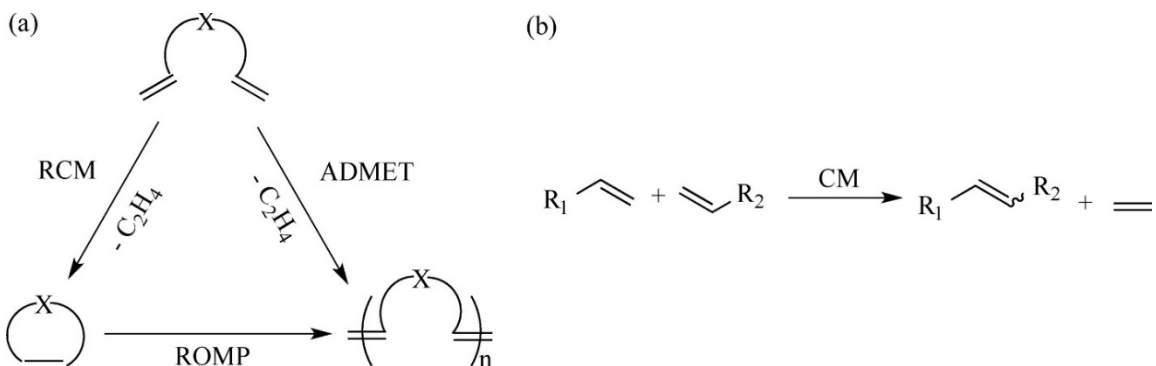


Figure 1. Categories of olefin metathesis reactions. (a) Ring-closing metathesis (RCM), ring-opening metathesis polymerization (ROMP), acyclic diene metathesis (ADMET), and (b) cross-metathesis (CM). Figure reproduced from reference 9.

Each category of olefin metathesis transformation can be described by its energetic driving force and potential applications. For example, RCM and ROMP are primarily driven by entropy and ring-strain release, which results in irreversible reactions.¹⁰ CM and ADMET lack entropic driving forces and enthalpic barriers; therefore removing ethylene, one of the products in these reactions, is essential to control reaction direction.^{11, 12} These differences make OM amenable to multiple applications; e.g., RCM is commonly used in natural product synthesis,¹³⁻¹⁶ ROMP and ADMET are applied to medical materials with biological properties,^{7, 8, 17, 18} and CM is utilized for asymmetrical organic synthesis in pharmaceutical applications.¹⁹

1.2 Chauvin Mechanism

As mentioned previously, Chauvin mechanism is the most acceptable mechanism of OM reaction which is strongly supported with experimental evidence, proposed in 1971.²⁰ It states that the metal carbene (metal alkylidene) is the active site, and metallocyclobutane is the crucial intermediate in the catalytic cycles (Figure 2).⁷ One cycle includes two steps of [2+2] cycloadditions for targeting product formation.

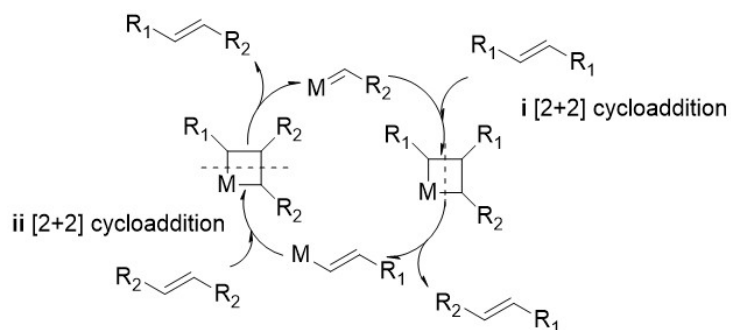


Figure 2. Chauvin mechanism of olefin metathesis.

- i. A metal carbene on the catalyst reacts with one olefin and forms a metallacyclobutane, consisting of one metal atom and three carbons. Two of the bonds on the metallacyclobutane are then cleaved, forming an olefin product and a new metal carbene.
- ii. The new metal carbene is involved in the same cycloaddition with another olefin, then the target olefin product forms. The metal carbene starts a new catalytic cycle.²¹

Since several experimental data supported this mechanistic proposal, it laid the foundation for later OM catalyst design.²¹

1.3 Catalyst Development

The most desirable catalysts used in olefin metathesis reactions are homogeneous catalysts, which can be dissolved in the same phase as reactant molecules and have easier accessible active sites than solid-state heterogeneous catalysts.²² Schrock- and Grubbs-type catalysts are the most popular and well-defined homogeneous systems with high efficiencies. Unlike early multicomponent, heterogeneous catalytic systems composed of titanium or tungsten salts and alkylating agents, Schrock- and Grubbs-type catalysts do not require harsh reaction conditions are compatible with varying functional groups, and results in less side reaction. Both systems include $L_nM=CR_2$ type metal carbene complexes, and the variations of metal centers and ligands largely influence catalyst characteristics.^{7, 23}

Generally, the characteristics of catalysts include the induction time for initiation, stability, and tolerance of functional groups. Induction time is the period activate the metallic carbene at the beginning of catalytic cycles. A short induction time (high initiation rate) leads to higher activity in metathesis reactions. The induction time is prolonged with more bulky protecting groups around the metal center. The catalyst stability is mainly related to the metal center. If the metal has high oxophilicity, such as tungsten and molybdenum, renders high sensitivity to air and water and shows instability in the reactions. A stable catalyst presents a longer lifetime and higher overall efficiency.^{24,25} Eventually, the tolerance of functional groups is determined by both the metal center and ligands on the catalysts.²⁶

1.3.1 Schrock Catalyst

The first well-defined catalyst, Schrock molybdenum-based and Lewis acid-free catalyst was synthesized for OM, published in 1986 by Richard R. Schrock and co-workers (Figure 3a).²⁷ The alkylidenes stabilize Mo (VI) in the general form of $[\text{Mo}(=\text{CHMe}_2\text{Ph})(=\text{N-Ar})(\text{OR})_2]$. This electron-deficient nature of the metal center withdraws electrons from the ligands and increases the complex electrophilicity, which increases the catalyst activity.²⁸ It is a double-edged sword for the catalyst. The high activity and no adverse side reactions are highly efficient in ring-closing reactions and polymer brush synthesis. However, the active catalyst is sensitive to water, oxygen, and high temperature, limiting potential substrates. Compared with later, more versatile catalysts, it has less tolerance of polar functional groups.^{1, 6, 8, 29}

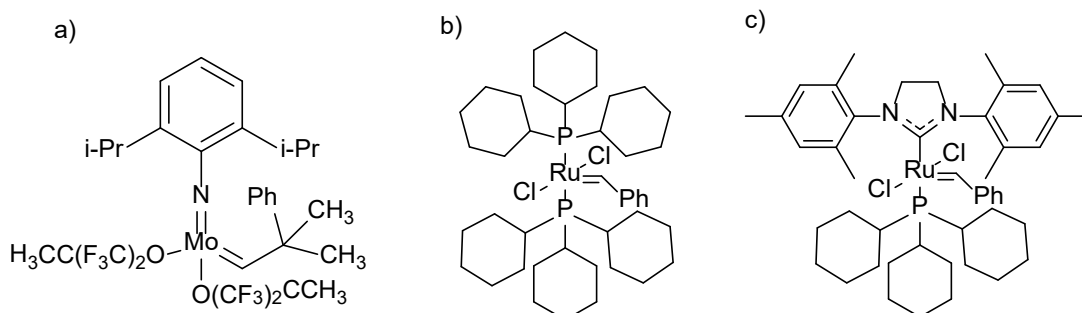


Figure 3. Common homogeneous metathesis catalysts (a) The first reported Schrock catalyst, (b) First, and (c) second generation Grubbs catalysts.

1.3.2 Grubbs Catalyst

Another group of well-defined catalysts for olefin metathesis reactions is Grubbs ruthenium-based catalyst, designed by Robert H. Grubbs and co-workers.³⁰ Starting from the 1960s, ruthenium salts were used to catalyze aqueous ROMP reactions and presented low activity because of prolonged reduction time. The ligands were modified in the symmetric form of $[L_2X_2Ru=CHR]$ to improve the initiation behavior.²³ The first generation of Grubbs catalyst (G1) used chloride as X-type and tricyclohexylphosphine (PCy_3) as L-type ligands in the complex (Figure 3b). PCy_3 as the primary phosphine leads to shorter reduction time and higher activity than the ill-defined systems, and the polymer product molar mass dispersities are narrower in ROMP reactions.⁷ Since ruthenium reacts preferentially with double bonds on olefins and presents more stability than molybdenum, it displays greater tolerance of functional groups than previous catalyst systems and is still effective in the presence of groups such as aldehydes, alcohol, and carboxylic acids.²⁵

However, G1 does not present the same efficiency in other OM transformations, such as CM of electron-deficient olefins.⁹ To enhance the catalyst activity, one of the PCy_3 ligands can be replaced by an N-heterocyclic carbene (NHC) ligand, to form the second generation of Grubbs catalysts (G2) is formed (Figure 3c). Compared to PCy_3 , NHC has strong σ donor ability and

high binding ability to π -acidic olefin. This modification increases the dissociation of the remaining PCy₃ ligand, which improves the catalyst reactivity and metathesis activity. G2 keeps similar properties as G1, broad tolerance of air, water, and functional groups, and enables more synthesis of OM transformations.¹⁹ Continuously, Grubbs and co-workers adjusted the design of ruthenium-based catalysts by exchanging the second PCy₃ ligand to other L-type donors (e.g., 3-bromopyridines) or altering the NHC substituents to achieve higher thermal stability, reactivity, and selectivity.^{7, 25}

1.4 ADMET Polymerization

As the catalysts became more effective in OM, more transformations was explored; acyclic diene metathesis (ADMET) polymerization is one of them.³¹ Initially, Wagener and co-workers used an ill-defined catalytic system, WCl₆/EtAlCl₂, which came with unavoidable vinyl additions as side reactions.³² Using Schrock molybdenum-based catalytic system, high molecular weight polymers could not be synthesized via ADMET polymerization.³³ Unlike ROMP, ADMET polymerization is a step-growth condensation reaction and shares the same mechanism as CM.³⁴ It is used to synthesize unsaturated linear polymers in either bulk or solution conditions.¹⁷ The saturated versions of these polymers can be accessed via post-polymerization modification by hydrogenation.³⁵

1,9-decadiene was the first monomer successfully polymerized via ADMET polymerization into polyoctenamer in 1991.³⁶ From then on, ADMET was explored and used to polymerize symmetric α,ω -dienes to form products with regiochemical specificity, because it favors only one of the possible metallocyclobutane formations, α,β substitutions, based on the steric profile of the olefin.³³ Thus, ADMET distinguishes itself relative to ROMP by consistently allowing access to polymers with well-defined primary structures (high uniformity of carbon spacing and frequency in the backbone) and precision placement of substituents of the backbone. The

primary structure affects the properties of the polymer in melting transition, crystallinity, and other parameters.³⁷⁻³⁹ Therefore, ADMET provides a vital ability to control polymer morphology and thermal behavior.

1.4.1 ADMET Polymerization Conditions

Because of the step-growth nature of ADMET polymerizations, certain conditions are needed to achieve effective catalysis. The most important of these appears to be a high vacuum system to remove ethylene, a gaseous byproduct of the reaction, and drive the reaction equilibrium towards forming polymers. Similarly, a long reaction time is required to achieve high molecular weight polymers, and a catalyst with a prolonged lifetime keeps efficient.⁴⁰ The reaction progress can be observed by comparing the integrations of the NMR peaks indicative of terminal olefins on the monomers with those indicative of internal olefins in the unsaturated polymer chains.^{29, 32,}
⁴¹ Bulk or solution conditions also influence the yield. Under bulk polymerization conditions, the catalyst is dissolved in the liquid monomer as the solvent for the reactions. This setup is more convenient than solution conditions, and less cyclization is observed.⁴² Rigorous stirring and heating are necessary for effective diffusion and driving off ethylene during reactions using bulk conditions.⁴⁰

1.4.2 Applications

ADMET polymerization is often used to synthesize functionalized polyethylene (PE) that have potential applications in material and medical fields. PE, the highest produced volume polymer, can be made with precisely placed pendent groups every certain number of carbons on the backbone via ADMET conditions. Reported branch identities of functional PE include alkyl groups, halogens, and carboxylic acids.⁴³ More special applications of ethylene copolymers are also possible via ADMET, such as ethylene-co-aryl ether polymers as electroactive materials and polymers incorporated sulfonic acid for ion-transport.⁴⁴ ADMET can be used to synthesize

hyperbranched polymers with multiple end groups for nanoscale drug or gene delivery, which includes high solubility and low viscosity in solutions, compared to linear analogues.⁴⁵ Some polymeric prodrugs include variations of pendant groups as molecules releasing platforms. The drug or prodrug release is controlled via differing polymer solubility and chain collapse.³⁷ ADMET is good at making model systems for these applications and allows to learn the structure property relationship.

1.4.3 Drawbacks

Even though ADMET has been applied in various areas, several drawbacks limit the potential applications of ADMET. In ADMET polymerization conditions, high vacuum and elevated temperature are required for removing ethylene and reaching monomer melting points, which results in solution vaporization so there are fewer solvent options for polymerization.⁴⁶ Moreover, unwanted products may be produced by isomerization when the catalyst is too active and easily degraded.⁴⁷ In addition, ADMET is limited to synthesizing alternating oligomers or copolymers, because olefins with high reactivity form the active internal olefins on the backbone.³⁷ This phenomenon results in random statistical copolymers.

1.5 SADMET Polymerization

To synthesize alternating copolymers via ADMET polymerization for more potential applications, we introduce Selective Acyclic Diene METathesis (SADMET) polymerization (Figure 4) which is based on prior study of ring-opening insertion metathesis polymerization (ROIMP) and alternating diene metathesis (ALTMET).^{48, 49} In 2002, Grubbs and co-workers successfully used ROMP to synthesize AB alternating copolymers and observed that diacrylates were selectively inserted into poly(1-octene) after rapid ROMP.⁴⁸ Given the limited sources of cyclic monomers for ROIMP, Galli and co-workers synthesized similar AB alternating copolymers with ADMET polymers and named it ALTMET.⁴⁹ Different from ALTMET

synthesis of diene and diacrylate alternating copolymer, we are introducing SADMET polymerization as a new method to synthesize alternating copolymer with new functional groups, using selective reactivity of olefins and catalysts. SADMET polymerization includes two processes (Figure 4): a) synthesis of a homopolymer via primary ADMET polymerization and b) synthesis of the alternating copolymer via secondary SADMET polymerization.

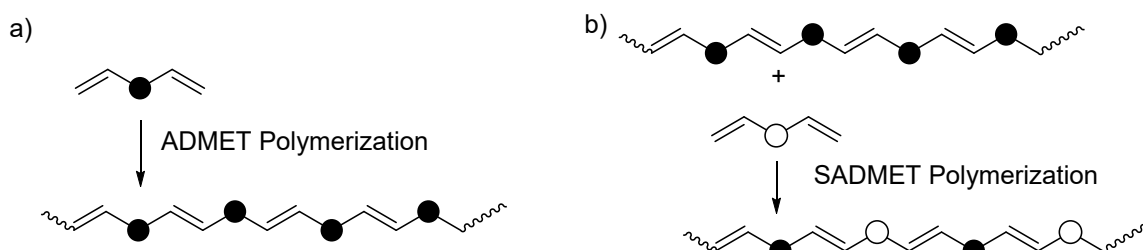


Figure 4. Synthesis of alternating copolymers via a) primary ADMET polymerization and b) secondary SADMET polymerization.

1.5.1 Olefins Categorizations

SADMET is a step growth polycondensation with AA (Type I) and BB (Type II/III) type monomers and is technically easier than polymerization of AB monomers.⁵⁰ Identifying olefin reactivity is crucial to synthesize alternating copolymer via SADMET. Chatterjee and co-worker set a general model for selectivity in CM and observed self-metathesis and CM to categorize olefin reactivity.⁵⁰ Applying this model to SADMET polymerization, a slower rate of homopolymerization would help control copolymerization between active olefins and less active ones. Therefore, we define four categories of olefins for SADMET that are analogous to the four types in Chatterjee work on CM. Type I olefins are most active and rapidly homopolymerized under ADMET conditions, like terminal olefins. Type II olefins homopolymerize at a slower rate or undergo cross metathesis such as acrylates and acrylic acid olefins. Type III cannot be homopolymerized but undergo copolymerization with Type I/II olefins, including 1,1-

disubstituted olefins. Type IV olefins are unreactive to metathesis such as disubstituted α,β -unsaturated carbonyl. As Type I olefins rapidly homopolymerize under ADMET conditions, Type II/ III olefins can be ideally inserted into the homopolymer via SADMET polymerization to achieve alternation.

Table 1. Categorization of olefins for SADMET polymerization.

Olefin type	Reactivity	Homopolymerization	Copolymerization
Type I	Most reactive	React at a rapid rate	Statistical copolymer with Type I
Type II	↓	React at a slow rate	Alternating copolymer with Type I
Type III		Do not react	Alternating copolymer with Type I/II
Type IV		Least reactive	Do not react

1.5.2 Research Goal

The goal of this research project has been to find Type II and III olefins, which can be used to synthesize alternating copolymers under SADMET conditions; with a 1:1 moiety ratio between active (Type I) and less active (Type II/III) olefins. Olefin reactivity is dependent on electronic and steric effects. The electron-rich and sterically unhindered olefin is more active than the electron-deficient and sterically bulky olefin. Therefore, we hypothesize that Type II and III olefins can be designed by changing either the electronic or steric of the olefin. We will focus on steric effect in this research.

More factors, included in this research, are the choices of functional groups and catalysts. Altering functional groups on the backbone can tune the resultant polymer properties, and finding new functional groups, like polyesters, polyamides, and polyethers will provide more options of future applications. In previous studies, we synthesized olefins with ester or amide functional groups, so we will now explore ether-containing monomers. The choice of catalyst affects olefin reactivity in the polymerization reactions by varying their activity and tolerance of functional groups. Grubbs catalysts are better choices than Schrock catalyst because of their greater compatibility with a variety of functional groups and the ability to handle them in air and water with simple drying and degassing processes. Herein we use commercially available G1 and G2 are examined under the same reaction conditions to explore more Type II and III olefins.

Synthesis of Monomers

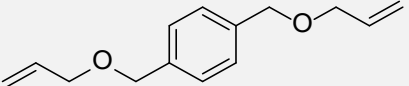
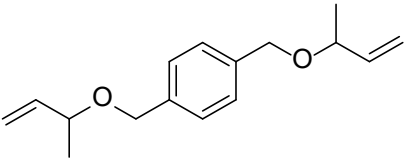
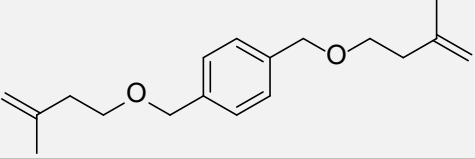
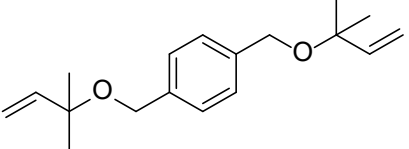
2.1 Background

Primarily olefins with various functional groups can be used to desirable polymers. As mentioned above, we have previous studied ester- and amide-containing monomers with an emphasis on using electronic effects to achieve selectivity. Now we explore steric effects on selectivity with ether-containing olefins under SADMET polymerization conditions. Ether functional groups in the polymer backbone could be applicable to polymers for ion-transport, drug delivery, and self-assembly.

The monomers are designed symmetrically, and the same number of carbons are placed on both sides of the aromatic ring, which is better to control the spacing between functional groups in the resultant polymers.⁵¹ The benzyl ether olefins can be used to degrade polymer and thereby quantify alteration of polymers in future work. All monomers are synthesized from the same aromatic diol with various allylic alcohols, allowing for the conversion of the diols into α , ω -dienes by etherification.^{52, 53}

The four monomers (**M1-M4**) that we have designed differ in terms of steric environment around the alkene and are expected to be classified into different reactivity categories (Table 2). **M1-M4** are 1,4-bis[(2-propen-1-yloxy)methyl]benzene (**M1**), 1,4-bis[[1-methyl-2-propen-1-yl)oxy]methyl]benzene (**M2**), 1,4-bis[[3-methyl-3-buten-1-yl)oxy]methyl]benzene (**M3**), and 1,4-bis[[1,1-dimethyl-2-propen-1-yl)oxy]methyl]benzene (**M4**). We hypothesize that the amount of steric hindrance will tune the monomer reactivity from high reactivity in **M1** to low reactivity in **M4** based on having more substituents on the double bond carbons or the adjacent carbon.

Table 2. Four α, ω -diene monomers designed and synthesized for this project.

Monomer	Structure	Steric Hindrance	Reactivity
M1		Low	High
M2		↓ High	↓ Low
M3			
M4			

2.2 Material and Methods

2.2.1 General Information

Thin-layer chromatography (TLC) was performed with silica gel 60 F254 plates (0.25 mm thickness) and was imaged with iodine as an indicator. Column chromatography was performed with silica gel 60 (40-60 μm) from Acros Organic. All other materials were purchased from Sigma Aldrich. Commercial compounds were used without further purification. All synthesized monomers were analyzed by nuclear magnetic resonance (NMR) spectroscopy on a Bruker 300 MHz spectrometer with CDCl_3 as the solvent and referencing the internal residual solvent peak to 7.26 ppm.

2.2.2 Representative Procedure

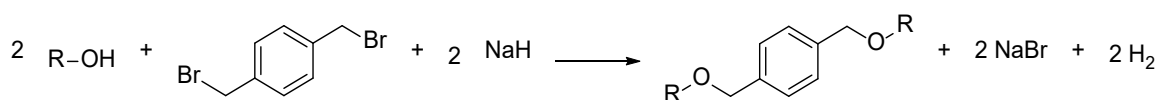
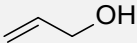
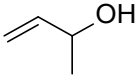
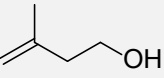
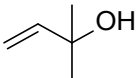


Figure 5. General model for monomer synthesis.

All monomers were synthesized via Williamson Ether Synthesis using air-free techniques (Figure 5). The synthesis includes two parts: (1) deprotonation of the alcohol with sodium hydride and (2) an S_N2 reaction of dibromo benzene with deprotonated alcohol. The round bottom flask, including a stir bar, was connected to Schlenk line and flame-dried under vacuum. Excess sodium hydride (60% suspension in oil, 50 mmol) was added to the flask under positive nitrogen flow, and 200 mL of dry tetrahydrofuran (THF) was transferred via cannula. The resulting suspension was cooled to 0 °C in an ice bath. The appropriate alcohol for the target monomers (40.0 mmol, see Table 3) was added into the reaction flask and the mixture was stirred for 30 minutes. 1,4-bis(bromomethyl)benzene (20.0 mmol) was added in under positive pressure, and the mixture was heated to 60 °C for 24 hours.

Table 3. Alcohol starting materials for monomers M1-M4.

Monomer	Type of Alcohol	Alcohol
M1	1° Allylic	
M2	2° Allylic	
M3	1,1-disubstituted	
M4	4° Allylic	

To purify each monomer, 200 mL 1M hydrochloric acid was added to the mixture, and the organic layer including the target product was extracted with 200 mL dichloromethane (DCM) three times. The collected organic layer was dried with magnesium sulfate and gravity filtered to access a clear, colorless solution that was then concentrated to yield the crude product. The crude product was analyzed by NMR spectroscopy. If there were impurities, the crude product was purified through the column chromatography after the solvent system was determined by TLC.

2.3 Result

2.3.1 M1 (1,4-Bis[(2-propen-1-yloxy)methyl]benzene)

The amounts used for **M1** were as follows: 60% sodium hydride (4.6 g, 190 mmol), 2-propen-1-ol (2.4 g, 41 mmol), and 1,4-bis(bromomethyl)benzene (5.0 g, 19 mmol). The crude **M1** product was purified using column chromatography with 9.5:0.5 hexane: ethyl acetate as the eluent. **M1** was isolated as a yellow liquid in 63% yield (2.5 g). All proton peaks and multiplets are labelled in the ^1H NMR spectrum below (Figure 6). In the ^{13}C NMR spectrum (Figure 7), the alkene carbons are seen at 134.69 and 117.11 ppm, the aromatic carbons are at 137.64 and 127.79 ppm, and peaks at 71.84 and 71.05 ppm are ether carbons.

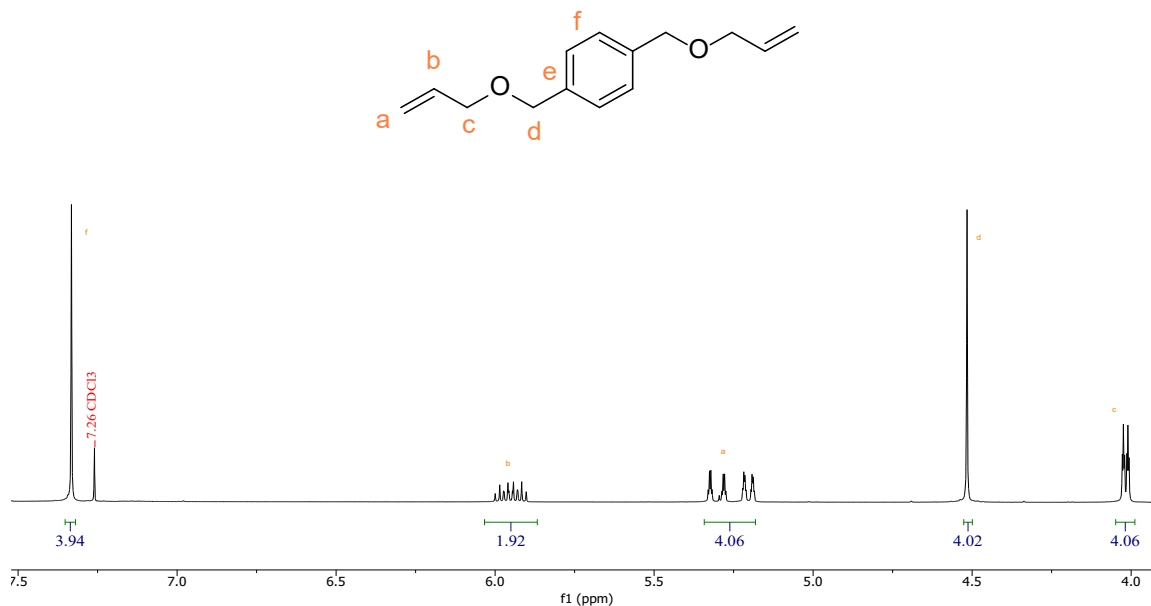


Figure 6. ^1H NMR spectrum of M1.

^1H NMR (400 MHz, Chloroform-*d*) δ 7.33 (aromatic, s, 4H), 5.95 (olefinic, ddt, $J = 17.2, 10.3, 5.6$ Hz, 2H), 5.43 – 5.09 (olefinic, dd, 4H), 4.52 (benzylic, s, 4H), 4.02 (allylic, dt, $J = 5.6, 1.4$ Hz, 4H).

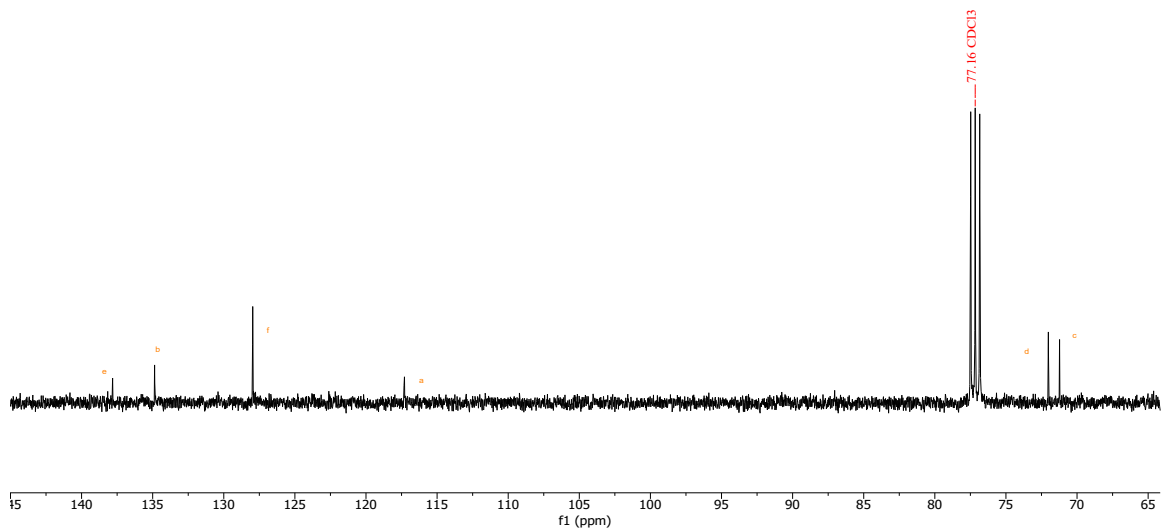


Figure 7. ^{13}C NMR spectrum of M1.

^{13}C NMR (101 MHz, Chloroform-d) δ 137.64, 134.69, 127.79, 117.11, 71.84, 71.05.

2.3.2 M2 (1,4-Bis[[1-methyl-2-propen-1-yl]oxy]methyl]benzene)

The amounts used for **M2** were as follows: 60% sodium hydride (5.0 g, 210 mmol), 3-buten-2-ol (2.8 g, 39 mmol), and 1,4-bis(bromomethyl)benzene (5.0 g, 19 mmol). The crude **M2** product was purified using column chromatography with 9.5:0.5 hexane: ethyl acetate as the eluent. **M2** was isolated as a yellow liquid in 65% yield (3.0 g). All proton peaks and multiplets are labelled in the ^1H NMR spectrum below (Figure 8), and two methyl groups are attached on allylic carbons, sharing same J constant. A small portion of THF can be observed in the spectra, and sample was further purified with rotavapor. In the ^{13}C NMR spectrum (Figure 9), the alkene carbons are seen at 140.41 and 116.24 ppm, the aromatic carbons are at 136.89, 128.71 and 127.69 ppm, peaks at 76.63 and 67.79 ppm are ether carbons, and methyl carbons are at 21.49 ppm.

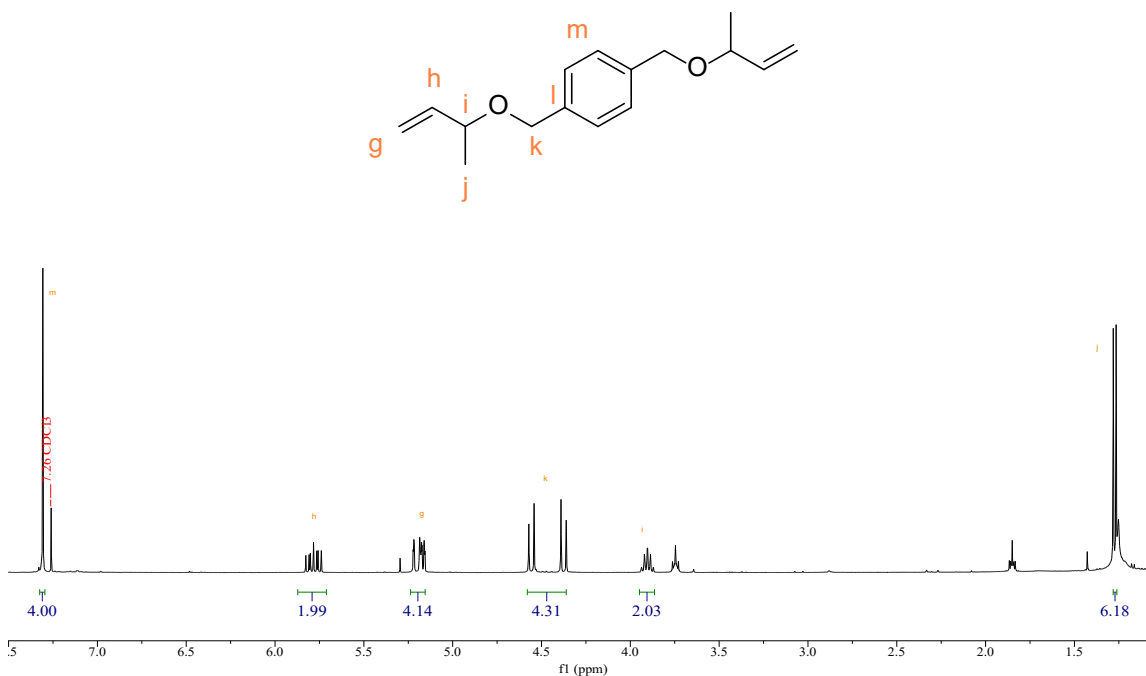


Figure 8. ¹H NMR spectrum of M2.

¹H NMR (400 MHz, Chloroform-d) δ 7.31 (aromatic, s, 4H), 5.78 (olefinic, ddt, 2H), 5.18 (olefinic, dd, 4H), 4.46 (benzylic, dd, 4H), 3.90 (allylic, dqt, $J = 7.3, 6.4, 0.9$ Hz, 2H), 1.27 (methyl, dd, $J = 6.4$ Hz, 6H).

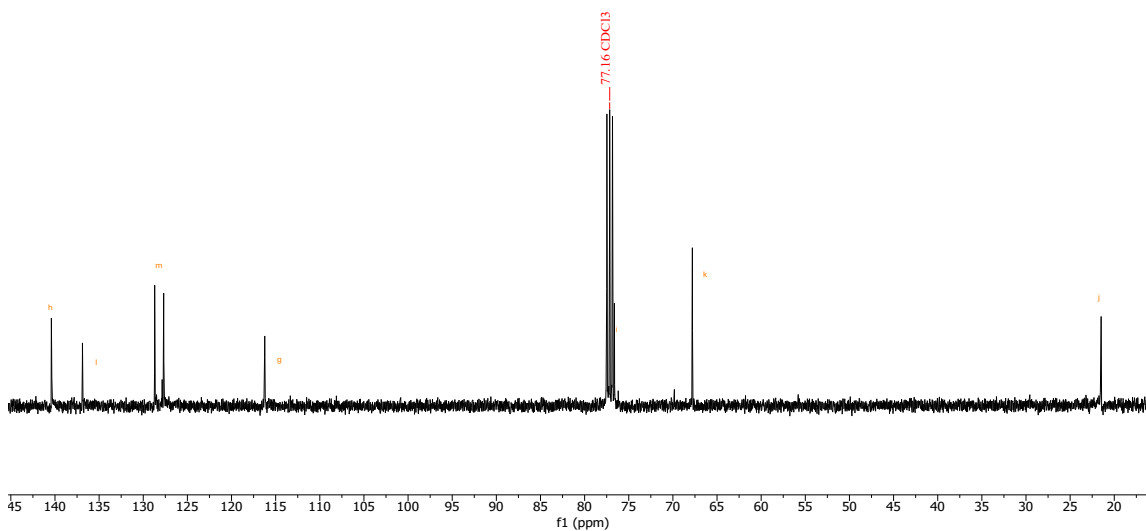


Figure 9. ¹³C NMR spectrum of M2.

^{13}C NMR (101 MHz, Chloroform-d) δ 140.41, 136.89, 128.71, 127.69, 116.24, 76.63, 67.79, 21.49.

2.3.3 M3 (1,4-Bis[[3-methyl-3-buten-1-yl]oxy]methyl]benzene)

The amounts used for **M3** were as follows: 60% sodium hydride (4.6 g, 190 mmol), 3-methylbut-3-en-1-ol (3.6 g, 42 mmol), and 1,4-bis(bromomethyl)benzene (5.0 g, 19 mmol). The crude **M3** product was purified using column chromatography with 9.5:0.5 hexane: ethyl acetate as the eluent. **M3** was isolated as a yellow liquid in 56% yield (2.9 g). All proton peaks and multiplets are labelled in the ^1H NMR spectrum below (Figure 10). In the ^{13}C NMR spectrum (Figure 11), the alkene carbons are seen at 142.94 and 111.52 ppm, the aromatic carbons are at 137.88 and 127.79 ppm, peaks at 72.74 are ether carbons, allylic carbons show at 68.71 and 37.87 ppm, and methyl carbons are at 22.75 ppm.

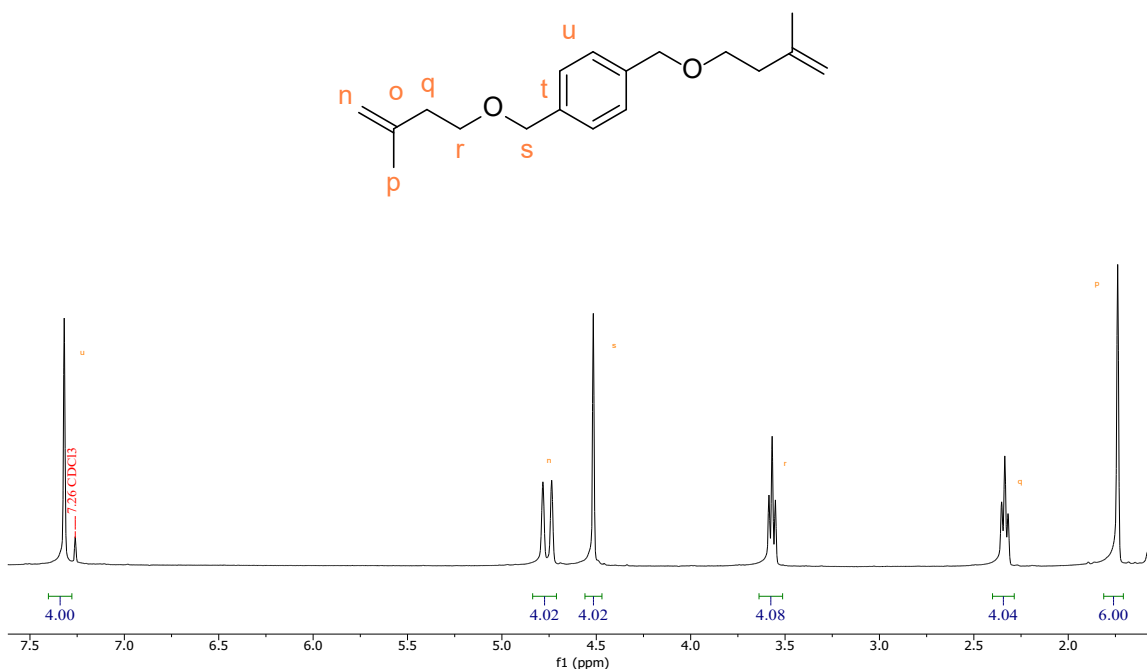


Figure 10. ^1H NMR spectrum of M3.

^1H NMR (400 MHz, Chloroform- d) δ 7.32 (aromatic, s, 4H), 4.76 (olefinic, d, $J = 18.5$ Hz, 4H), 4.52 (benzylic, s, 4H), 3.57 (allylic, td, $J = 6.9, 1.7$ Hz, 4H), 2.34 (allylic, td, $J = 7.0$ Hz, 4H), 1.74 (methyl, s, 6H).

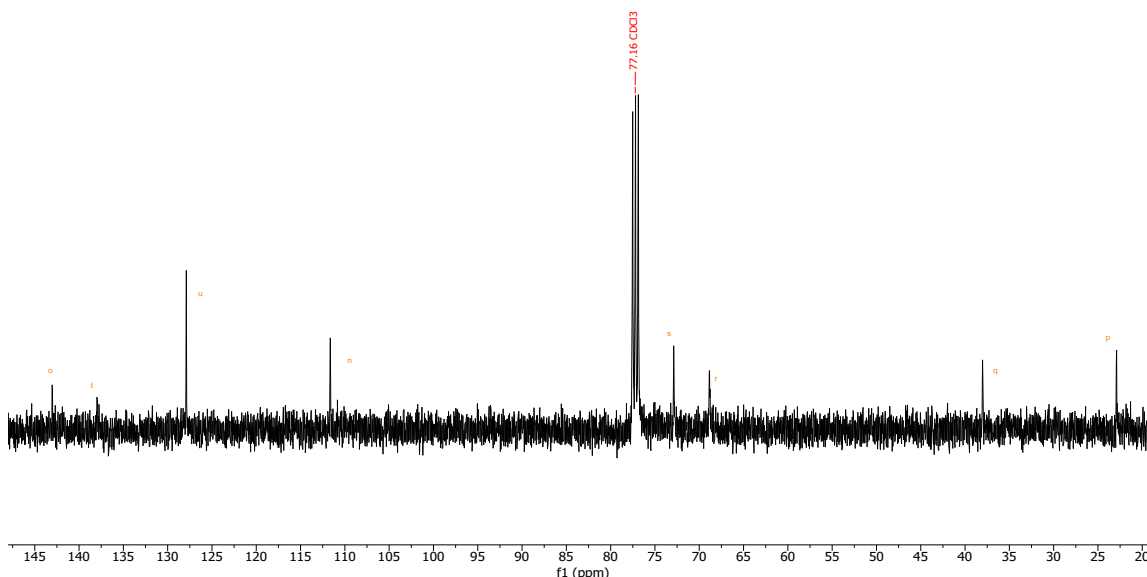


Figure 11. ^{13}C NMR spectrum of M3.

^{13}C NMR (101 MHz, Chloroform- d) δ 142.94, 137.88, 127.79, 111.52, 72.74, 68.71, 37.87, 22.75.

2.3.4 M4 (1,4-Bis[[1,1-dimethyl-2-propen-1-yl]oxy]methyl]benzene)

The amounts used for **M4** were as follows: 60% sodium hydride (4.6 g, 190 mmol), 3-buten-2-ol, 2-methyl (3.6 g, 42 mmol), and 1,4-bis(bromomethyl)benzene (5.0 g, 19 mmol). The crude **M4** product was purified using column chromatography with 9.5:0.5 hexane: ethyl acetate as the eluent. **M4** was isolated as a yellow liquid in 40% yield (2.1 g). All proton peaks and multiplets are labelled in the ^1H NMR spectrum below (Figure 12). A small portion of H_2O can be observed in the spectra. Water is hard vaporized via rotavapor, and sample was kept in vacuum oven overnight before used in further reactions. In the ^{13}C NMR spectrum (Figure 13), the alkene

carbons are seen at 144.10 and 114.06 ppm, the aromatic carbons are at 138.72 and 127.43 ppm, peaks at 75.75 and 64.94 ppm are ether carbons, and methyl carbons are at 26.12 ppm.

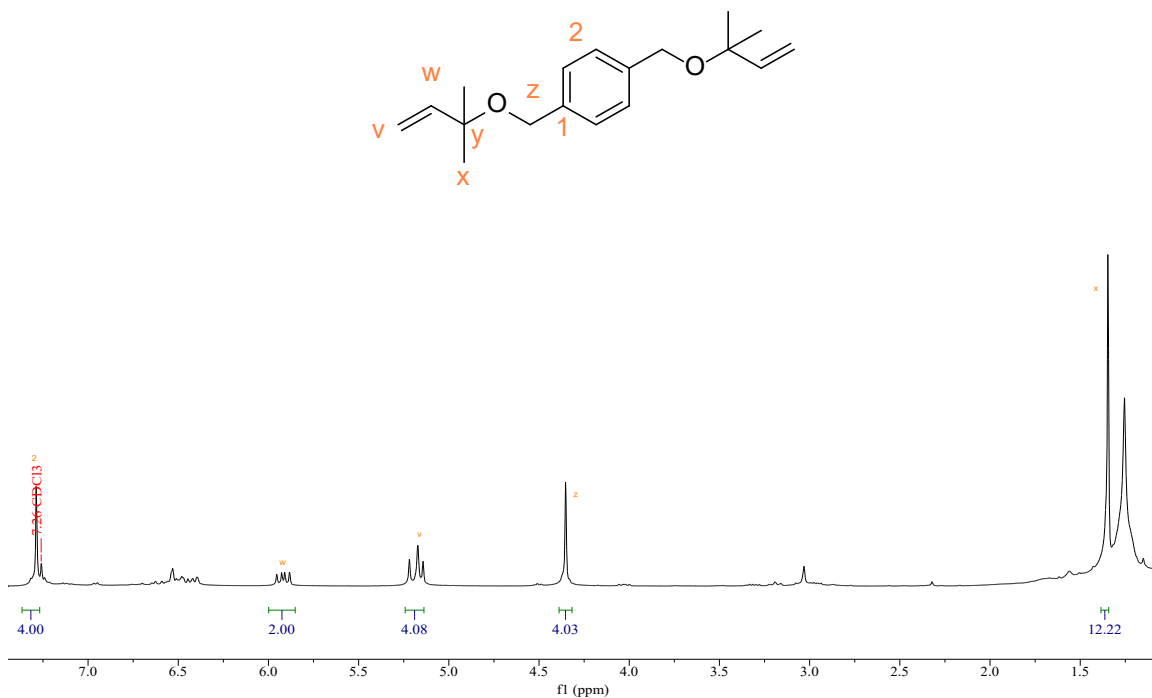


Figure 12. ^1H NMR spectrum of M4.

^1H NMR (400 MHz, Chloroform-*d*) δ 7.23 (aromatic, s, 4H), 5.86 (olefinic, dd, $J = 17.6, 10.8$ Hz, 2H), 5.11 (olefinic, td, $J = 8.8$ Hz, 4H), 4.29 (benzylic, s, 4H), 1.29 (methyl, s, 12H).

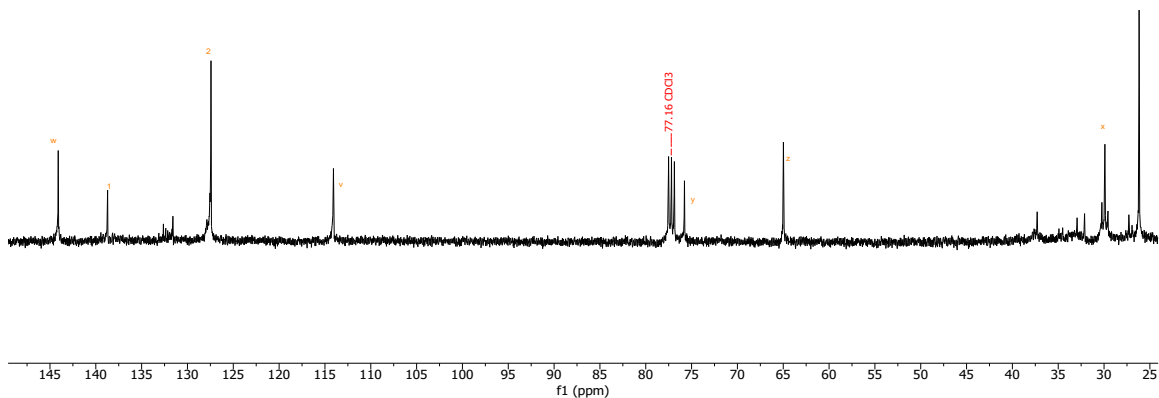


Figure 13. ^{13}C NMR spectrum of M4.

^{13}C NMR (101 MHz, Chloroform-*d*) δ 144.10, 138.72, 127.43, 114.06, 75.75, 64.94, 26.12.

2.4 Discussion

Four monomers (**M1-M4**) were made by Williamson ether synthesis. The impurities in crude products were removed via extraction and column chromatography. All products were isolated as yellow liquids in 40-65% yield. The structures were confirmed with ^1H and ^{13}C NMR spectroscopy. There are small portion of THF observed in **M2** and H_2O in **M4**. To prevent impurities influencing further polymerization reactions, we purified **M2** and **M4** via rotavapor and kept in vacuum oven overnight. Comparing with other three ether monomers, **M4** yields in the lowest percent of 40%. The lower yield was attribute to the higher steric hinderance level of **nucleophile** and increase the barrier of reaction with dibromo benzene.

With these monomers in hand, we can now study their reactivity under ADMET polymerization conditions, as well be described in Chapter 3.

Homopolymerizations

3.1 Background

After the four ether-containing monomers were successfully synthesized and purified (Chapter 2), their homopolymerization reactivity under ADMET conditions was analyzed (Figure 14). As detail in Chapter 1, Type I olefins will rapidly homopolymerized, and Type II will homopolymerize slowly resulting in only short oligomers. No homopolymerization will occur with either Type III or IV olefins. Since Type I olefin will produce statistical copolymers under SADMET conditions, we will only attempt the copolymerization of the olefins that are classified as Type II, III, or IV with 1,9-decadiene (see Chapter 4). Based on the steric profile of the monomers, we hypothesized that **M1** would act as a Type I olefin, **M2** would act as a Type I or II olefin, **M3** would act as a Type II or III olefin, and **M4** would act as a Type III or IV olefin.

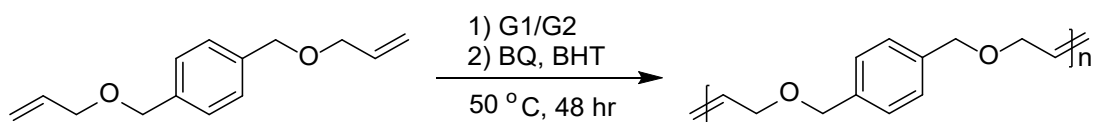


Figure 14. General ADMET homopolymerization reaction conditions.

There are some general considerations to achieve high catalyst efficiency and polymer yields under ADMET polymerization conditions. A high conversion maximizes polymer yields and molecular weight. Thus it is important to provide an environment that will not degrade the catalysts and that allows for a longer reaction time and optimized catalyst stability.⁴⁰ Grubbs 1st and 2nd generation catalysts, **G1** and **G2**, have high tolerance of functional groups and are used for the polymerizations herein. Because the catalyst longevity is affected by water and oxygen in the reaction, the use of air- and water-free techniques – including Schlenk tubes and a Schlenk line – are crucial for the polymerizations described herein. Typically, ADMET polymerizations

are run in bulk monomer. In bulk polymerization, the catalyst is dissolved in the monomer under a high vacuum, which helps remove the reaction byproduct, ethylene, from the reaction mixture.

One undesirable side reaction, olefin isomerization, has been observed with ruthenium-based initiators in ADMET polymerization, and a larger amount of isomerization occurs with G2 at elevated temperature. The unwanted isomers are difficult to separate from the desired products.⁴⁷ 1,4-benzoquinone (BQ) can be used as an additive to suppress isomerization by preventing the formation of ruthenium hydride complexes that catalyze the olefin migration that is responsible for side reactions. The isomerization makes the double closer to ether functional groups, poison to catalyst complexes.⁵⁴ We also employ a second additive, butylated hydroxytoluene (BHT), as an inhibitor to free radical oligomerization and to prevent spontaneous initiation and propagation. The free radical oligomerization causes cross-linking products and makes products insoluble.⁵⁵

3.2 Material and Methods

3.2.1 General Information

Both G1 and G2 were provided by Materia, Inc and Umicore. All other materials were purchased from Sigma Aldrich. Commercial reagents were used as received, without further purification. All GPC analysis was performed on a 1100 series HP instrument with Polymer Labs ResiPore columns as the stationary phase, tetrahydrofuran (THF) as the mobile phase, and an RI detector.

3.2.2 Representative Procedures

An oven-dried Schlenk tube with a stir bar was flame-dried to ensure removal of any condensation. Liquid monomer M (1.90 mmol) was injected through a long syringe into the bottom of the tube so as to avoid any monomer ending up on the sides of the tube and thus not getting polymerized. The tube was placed under vacuum to degas the monomer and then

backfilled with N₂ before adding the solid reagents: G1 or G2 (0.03 mmol, 2% catalyst loading relative to monomer), BQ (25 mg, 0.23 mmol), and BHT (50 mg, 0.23 mmol). Ethylene bubbles formed immediately. The sudden surge of large bubbles may spill the reactants, and intermittently vacuum was applied to avoid losing material on the sides of the tube. Full vacuum was applied when the mixture began to bubble vigorously. The mixture was heated to 60°C and stirred to 48 hours. After that, the reaction mixture was cooled to room temperature and quenched with 0.3 mL ethyl vinyl ether and 2-3 mL of toluene. Polymer products were precipitated by dropwise addition of the reaction mixture into 200 mL of old methanol and were collected via filtration. If no precipitation formed in cold methanol, the product mixture was concentrated by rotary evaporation. The product was dissolved in CDCl₃ for NMR analysis, and if a polymer structure had been observed, a second sample was dissolved in THF for GPC analysis.

After homopolymerization, the product was analyzed by NMR spectroscopy and gel permeation chromatography (GPC), a type of size-exclusion chromatography used to characterize polymers. GPC is a type of liquid chromatography that partitions the sample in the column based on size. The sample is prepared by dissolving the polymers in the mobile phase (THF was used for these samples), and the concentration of the sample should be 0.10% (weight/volume) for polymers with a molar mass between 10,000 and 1,000,000 g/mol. At this low concentration, the dissolved polymer chains will form individual coils in solution. Once the sample is prepared, it is filtered through a 0.22 μm fluorocarbon syringe filter and injected into the instrument where it will be pushed through the columns by the eluent. The columns contain the stationary phase with porous cross-linked polymer beads. Coiled polymers permeate in and out the porous molecules at different rates based on their sizes. The smaller molecules need more

time to elute from the column. The larger molecules need less time for the permeation, so the largest molecules elute first. After being detected by refractive index (RI) detector, the system characterizes the sample allowing for the calculation of mass average molecular weight (M_w), number average molecular weight (M_n), and dispersity (\mathcal{D}) by comparison to polystyrene standards of known molar mass and dispersity. Polystyrene is a reasonable standard for these polymers, since both have phenyl rings in the repeating unit.

3.3 Results

3.3.1 Homopolymerizations of **M1**

Two homopolymerizations of **M1** were attempted, one with each of the Grubbs catalysts (**G1** and **G2**). Following the general procedure above, **M1** (500 mg, 2.29 mmol) was combined with **G1** (25 mg, 0.03 mmol), BQ (25 mg, 0.23 mmol), and BHT (50 mg, 0.23 mmol). After the 48 h reaction time at 60 °C, the reaction was cooled and quenched, and the polymer products were precipitated as a black solid in yield 0.404 g and collected via filtration. Similarly, for the second homopolymerization attempt, **M1** (494 mg, 2.27 mmol) was combined with **G2** (20 mg, 0.03 mmol), BQ (25 mg, 0.23 mmol), and BHT (55 mg, 0.25 mmol). After the 48 h reaction time at 60 °C, the reaction was cooled and quenched, and the polymer products were precipitated as a black solid in yield of 0.422 g and collected via filtration.

The ^1H NMR spectrum of the precipitated material from the homopolymerization of **M1** with **G2** is shown in Figure 15, and protons on the internal olefin were detected at 5.80 ppm. GPC analysis was also carried out for both samples and showed that both polymerizations resulted in relatively short polymers: **M1** with **G1** resulted in a polymer with $M_n=5200$ g/mol and $\mathcal{D}=1.5$, while and **M1** with **G2** resulted in a polymer with $M_n=3800$ g/mol and $\mathcal{D}=1.7$. These data indicate that **M1** were homopolymerized with either **G1** or **G2** under ADMET polymerization conditions.

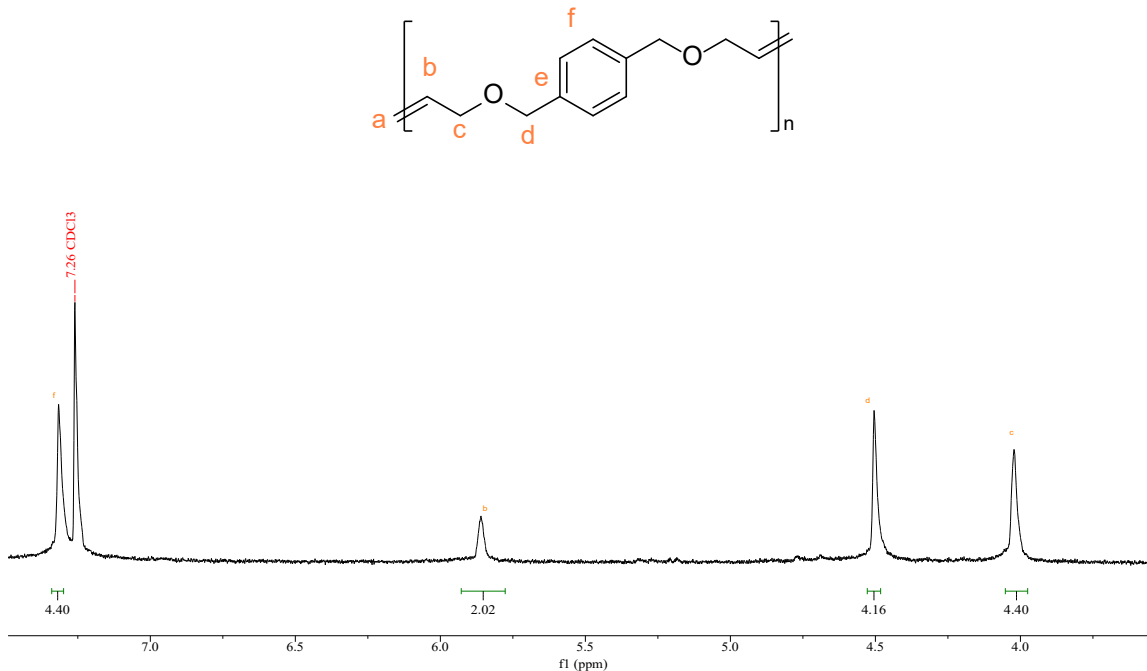


Figure 15. ^1H NMR spectrum of the homopolymerization of M1 with G2 as the catalyst.

^1H NMR (400 MHz, Chloroform- d) δ 7.20 (aromatic, s, $J = 2.2$ Hz, 4H), 5.80 (internal olefinic, s, 2H), 4.45 (allylic, s, 4H), 3.97 (allylic, s, 4H).

3.3.2 Homopolymerizations of M2

Following the general procedure above, **M2** (500 mg, 2.03 mmol) was combined with **G1** (25 mg, 0.03 mmol), BQ (23 mg, 0.21 mmol), and BHT (50 mg, 0.23 mmol). After the 48 h reaction time at 60 $^\circ\text{C}$, the reaction was cooled and quenched, and the polymer products were not precipitated and pump down as much solvent as possible via rotavapor. The collected product is a black liquid in yield of 0.465 g. Similarly, for the second homopolymerization attempt, **M2** (467 mg, 1.90 mmol) was combined with **G2** (24 mg, 0.04 mmol), BQ (26 mg, 0.24 mmol), and BHT (52 mg, 0.24 mmol). After the 48 h reaction time at 60 $^\circ\text{C}$, the reaction was cooled and quenched. The polymer products were precipitated as a black solid and collected via filtration in yield of 0.383 g.

The ^1H NMR spectrum of the product from the homopolymerization attempt of **M2** with **G1** is shown in Figure 16, and protons on terminal olefins are observed at 5.25 ppm, which means homopolymer was not formed under ADMET conditions. The ^1H NMR spectrum of the precipitated material from the homopolymerization of **M2** with **G2** is shown in Figure 17, and protons on the internal olefin were detected at 5.80 ppm. GPC analysis was also carried out with the precipitated material from this reaction, and the results indicated oligomers with $M_n=1800$ and $\bar{D}=1.8$. **M2** were oligomerized with **G2** under ADMET polymerization conditions.

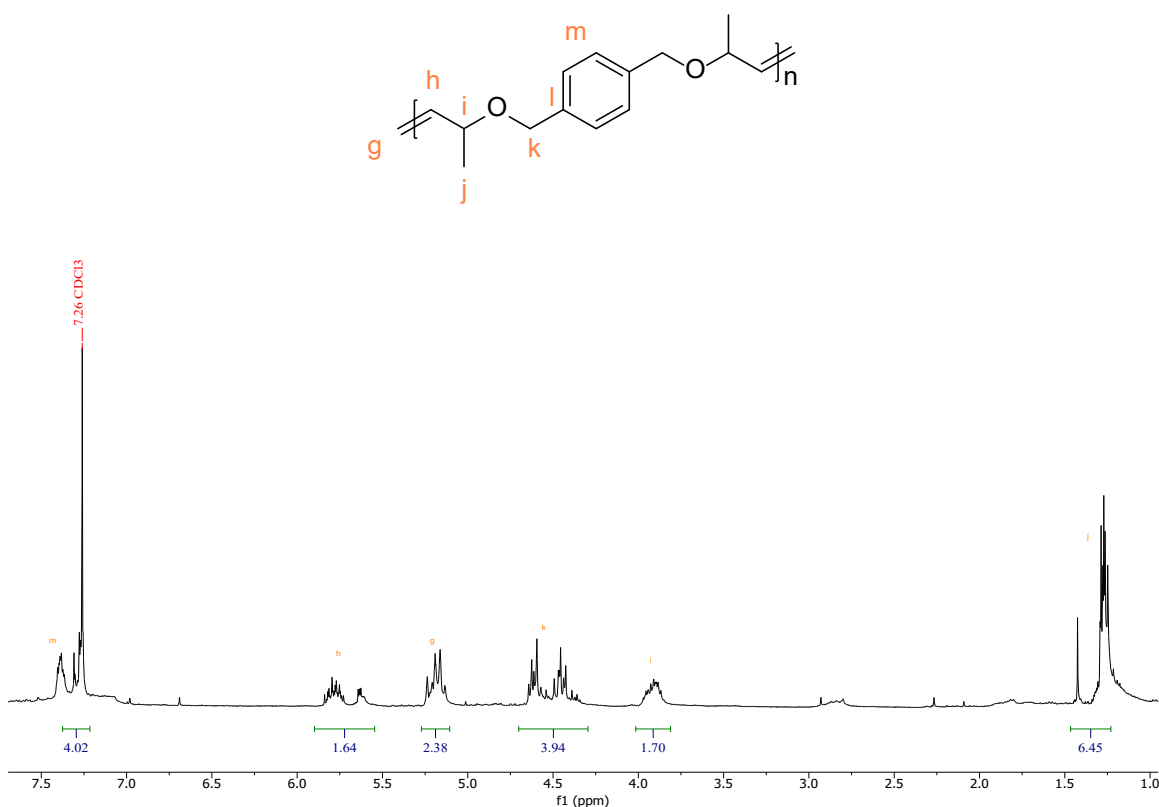


Figure 16. ^1H NMR spectrum of the homopolymerization attempt of **M2** with **G1** as the catalyst.

^1H NMR (400 MHz, Chloroform-d) δ 7.15 (aromatic, s, 4H), 5.65 (olefinic, td, 2H), 5.51 (olefinic, s, 2H), 5.06 (terminal olefinic, dd, 2H), 4.41 (allylic, ddt, 4H), 3.79 (allylic, td, 2H), 1.35 – 0.95 (methyl, m, 6H).

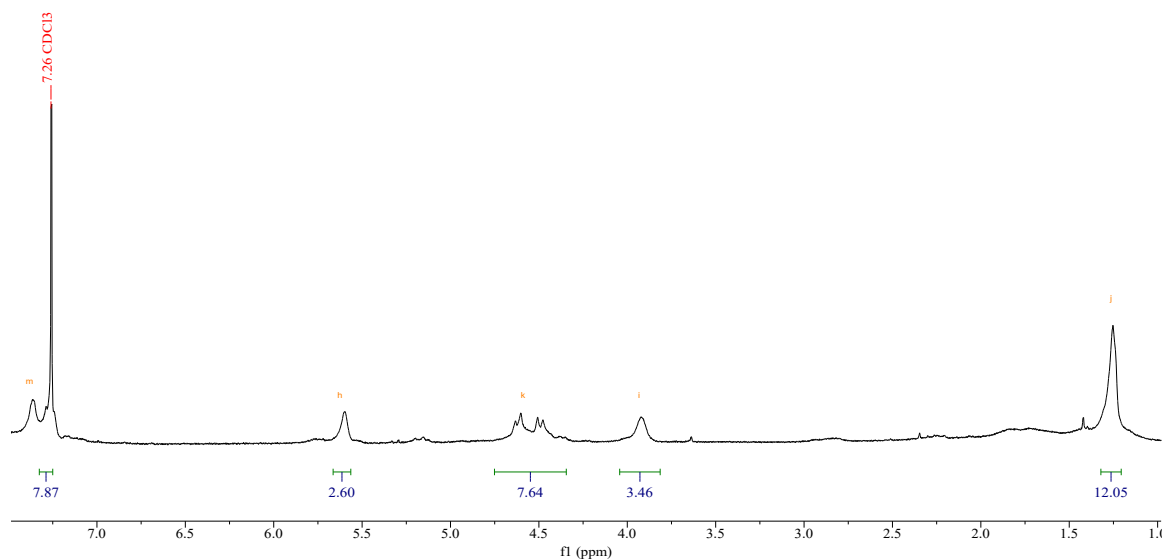


Figure 17. ^1H NMR spectrum of the homopolymerization of M2 with G2 as the catalyst.

^1H NMR (400 MHz, Chloroform-*d*) δ 7.34 – 7.19 (aromatic, s, 8H), 5.57 (internal olefinic, s, 2H), 4.53 (allylic, dd, $J = 48.4, 10.5$ Hz, 8H), 3.90 (allylic, s, 4H), 1.23 (methyl, s, 12H).

3.3.3 Homopolymerizations of M3

Following the general procedure above, **M3** (497 mg, 1.81 mmol) was combined with **G1** (24 mg, 0.03 mmol), BQ (26 mg, 0.24 mmol), and BHT (50 mg, 0.23 mmol). After the 48 h reaction time at 60 °C, the reaction was cooled and quenched, and the products were not precipitated and pump down as much solvent as possible via rotavapor. The product is a black liquid in yield of 0.472 g. Similarly, for the second homopolymerization attempt, **M3** (500 mg, 1.82 mmol) was combined with **G2** (24 mg, 0.03 mmol), BQ (25 mg, 0.23 mmol), and BHT (50 mg, 0.23 mmol). After the 48 h reaction time at 60 °C, the reaction was cooled and quenched, and the polymer products were not precipitated and pump down as much solvent as possible via rotavapor. The product is a black liquid in yield of 0.477 g.

The ^1H NMR spectrum of the product from the homopolymerization attempt of **M3** with **G1** is shown in Figure 18. The ^1H NMR spectrum of the product from the homopolymerization

attempt of **M3** with **G2** is shown in Figure 19. In both spectra, most protons peaks match **M3**, and protons on terminal olefins are observed around 4.80 ppm, which means homopolymer was not formed under ADMET conditions with **G1** and **G2**. There is small portion of methanol impurity in **M3** with **G2**.

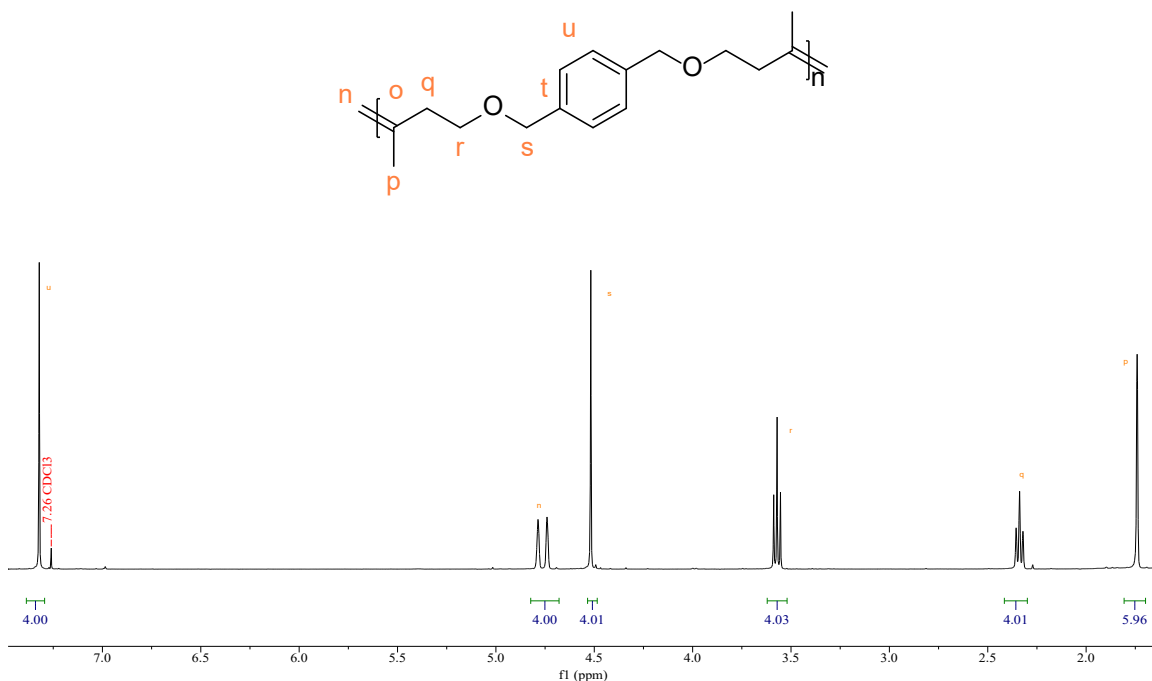


Figure 18. ¹H NMR spectrum of the homopolymerization attempt of **M3** with **G1** as the catalyst.

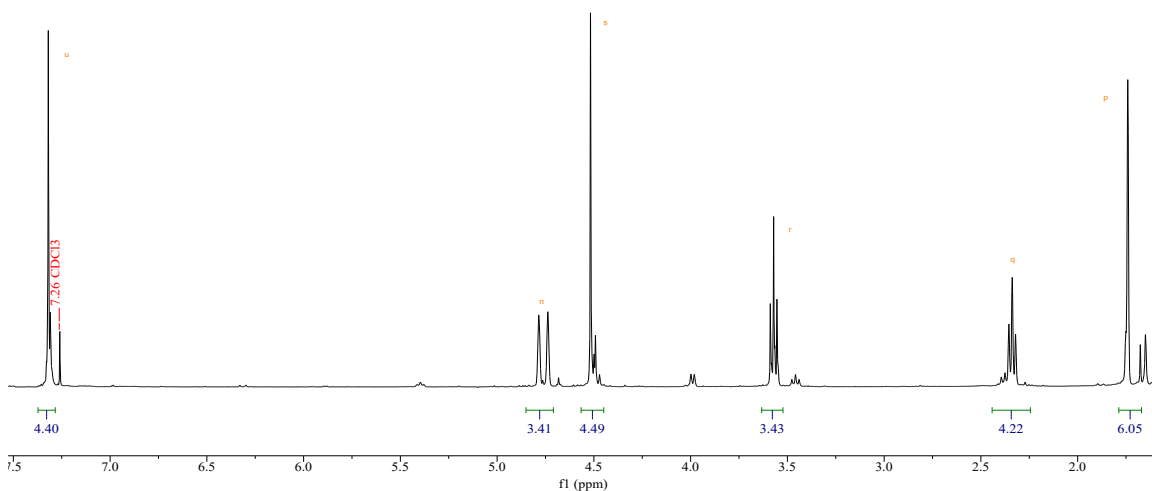


Figure 19. ¹H NMR spectrum of the homopolymerization attempt of **M3** with **G2** as the catalyst.

3.3.4 Homopolymerizations of M4

Following the general procedure above, **M4** (480 mg, 1.78 mmol) was combined with **G1** (23 mg, 0.03 mmol), BQ (24 mg, 0.22 mmol), and BHT (50 mg, 0.23 mmol). After the 48 h reaction time at 60 °C, the reaction was cooled and quenched, and the polymer products were not precipitated and pump down as much solvent as possible via rotavapor. The product is a black liquid in yield of 0.485 g. Similarly, for the second homopolymerization attempt, **M4** (384 mg, 1.42 mmol) was combined with **G2** (20 mg, 0.03 mmol), BQ (26 mg, 0.24 mmol), and BHT (40 mg, 0.18 mmol). After the 48 h reaction time at 60 °C, the reaction was cooled and quenched, and the polymer products were not precipitated and pump down as much solvent as possible via rotavapor. The product is a black liquid in yield of 0.485 g.

The ¹H NMR spectrum of the product from the homopolymerization attempt of **M4** with **G1** is shown in Figure 20. The ¹H NMR spectrum of the precipitated material from the homopolymerization of **M4** with **G2** is shown in Figure 21. In both spectra, peaks match **M3**, and protons on terminal olefins are observed around 5.20 ppm, which means homopolymer was not formed under ADMET conditions with **G1** and **G2**.

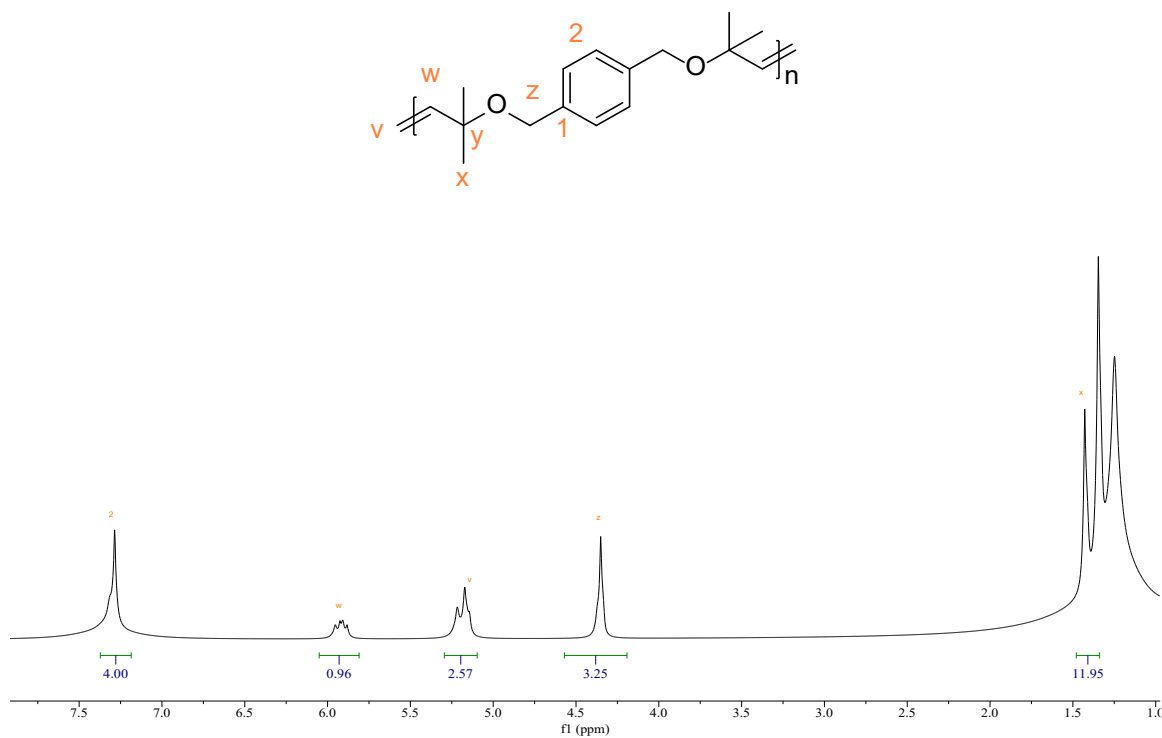


Figure 20. ¹H NMR spectrum of the homopolymerization attempt of M4 with G1 as the catalyst.

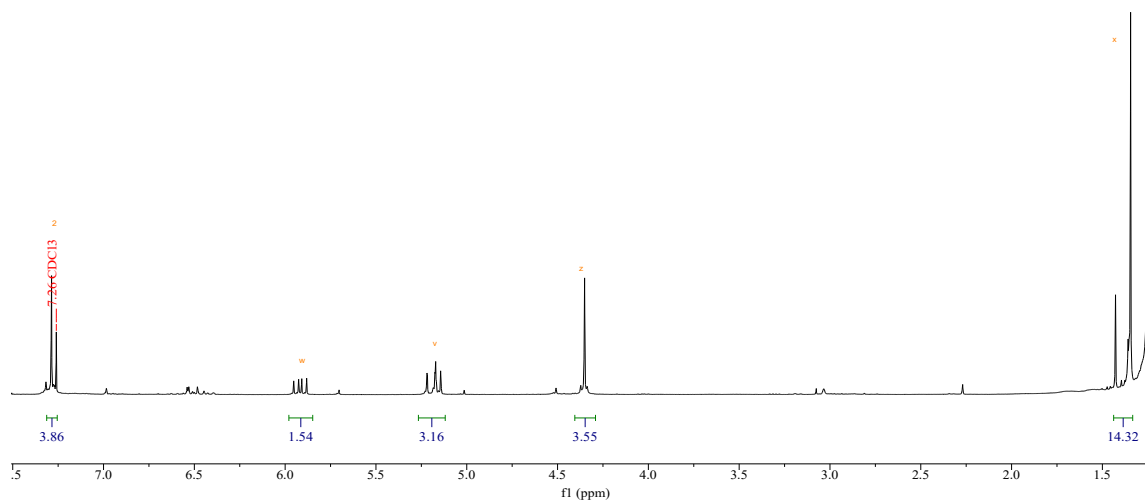


Figure 21. ¹H NMR spectrum of the homopolymerization attempt of M4 with G2 as the catalyst.

3.4 Discussion

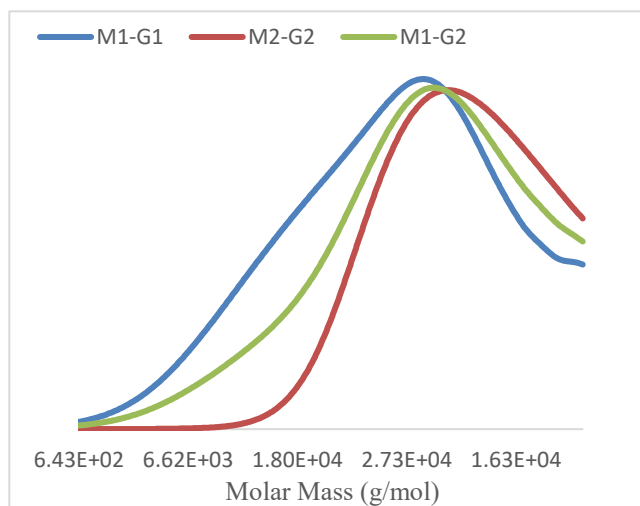


Figure 22. GPC analysis of homopolymer.

We attempted to homopolymerize our four olefins, **M1** – **M4**, with **G1** and **G2** under ADMET conditions, and GPC trace shows as Figure 22. **M1** is observed and classified as Type I olefin with both **G1** and **G2**, since the internal olefin is confirmed in NMR spectra. The terminal peaks present at the homopolymer of **M1** with **G1**. However, GPC data confirms the formation of homopolymer. Different from our expectation, **M1** with **G2** produce lower molecular weight polymer than **M1** with **G1**. It could cause by synthetic efforts. **M2** presents two classifications with **G1** and **G2**, which is related to catalyst activity. With the more active catalyst, **G2**, **M2** can be classified as a Type I olefin, which has oligomers formed after polymerization and internal olefin peaks in ^1H NMR spectrum. There is no homopolymer from in reaction of **M2** with **G1**, **M3**, and **M4** with **G1** and **G2**. Their reactivity will be classified after SADMET copolymerization in Chapter 4.

Copolymerizations with 1,9-Decadiene

4.1 Background

To further understand the impact the monomer steric profile on its reactivity, we attempted to copolymerize monomers **M2**, **M3**, and **M4** with 1,9-decadiene under SADMET polymerization conditions (1:1 moiety ratio between active and less active olefins) (Figure 23). As proposed in section 1.5, we expect to be able to selectively form alternating copolymers in reactions with monomers with significantly different reactivities. In SADMET, the active olefin (Type I) is rapidly homopolymerized, and then the less active olefin (Type II or III) is inserted in those homopolymers. In this work, 1,9-decadiene is used as a prototypical Type I olefin alongside our monomers which did not form homopolymer and are thus expected to be categorized as Type II, III, or IV. These experiments should allow full classification into the previously described categories: Types II, III, or IV. 1,9-decadiene was the first monomer polymerized using ADMET polymerization, and the reactivity under ADMET conditions is well known, classified as a Type I monomer with both **G1** and **G2**.³⁸ If **M2**, **M3**, and **M4** are Type II or III, they are expected to form alternating copolymers with 1,9-decadiene, but if they are Type IV, no incorporation will take place.⁵¹

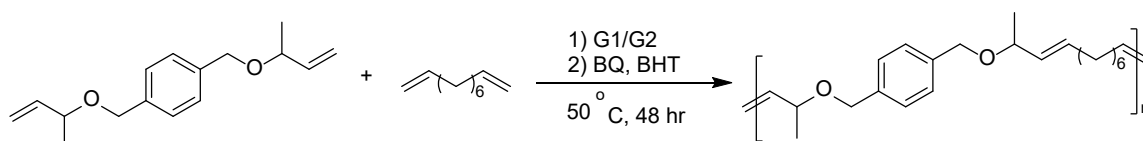


Figure 23. General scheme for copolymerization with 1,9-decadiene under SADMET conditions.

The resulting products from SADMET polymerization will be characterized with various NMR experiments, including 2D-NMR spectroscopy, specifically correlation NMR spectroscopy. Those spectra will allow us to determine the types of repeat unit sequences in the

polymer products. For example, a H-H COSY (CORrelation SpectroscopY) spectrum will have cross peaks that indicate a relationship between protons on adjacent carbons, which should be displayed symmetrically on both sides of the diagonal peaks in the spectrum.⁵⁶ Since a copolymer will have repeat sequence units, we can evaluate these sequences via peak analysis.⁵⁷

We hypothesize that 1,9-decadiene will react with Type II and III monomers and form alternating copolymers under SADMET conditions. In Chapter 3, **M1** with **G1** and **G2**, **M2** reacted with **G2** were classified as Type I with characterized homopolymers. Therefore, **M2** with less active catalyst, **G1**, is expected to form copolymer with 1,9-decadiene and classified as Type II or III. Because **M3** has more steric bulky, pendent groups closer to olefins, than **M1** and **M2**, it is expected to be type II or III. Likewise, **M4** is expected to be Type III or IV.

4.2 Material & Methods

4.2.1 General Information

Copolymerization was carried out using the same procedures as the homopolymerizations (see Section 3.2.2). 1,9-Decadiene was purchased from Sigma Aldrich and used as received. It was added to the reaction vessel via syringe at the same time as the other monomers.

4.3 Result

4.3.1 Copolymerization of **M2**

M2 (270 mg, 1.10 mmol) was combined with 1,9-decadiene(193 mg, 1.40 mmol), **G1** (25 mg, 0.03 mmol), BQ (26 mg, 0.24 mmol), and BHT (45 mg, 0.21 mmol). After the 48 h reaction time at 60 °C, the reaction was cooled and quenched, and the polymer products were precipitated and collected via filtration. The product is a black solid in yield of 0.285 g.

The ¹H NMR spectrum of the precipitated material from the copolymerization of **M2** with **G1** is shown in Figure 24. Peak 3 (5.55 ppm) and h (5.33 ppm) are protons on internal olefins, observed around 5.5 ppm, and there are small portion of terminal olefin at 5.2 ppm. Peak 3 and h

show correlation in COSY NMR spectrum (Figure 25). GPC analysis was also carried out with the precipitated material from this reaction and the results indicated a polymer with $M_n=8800$ g/mol and $\bar{D}=1.5$. These data are consistent with **M2** copolymerizing with 1,9-decadiene under SADMET polymerization conditions using **G1** as the catalyst.

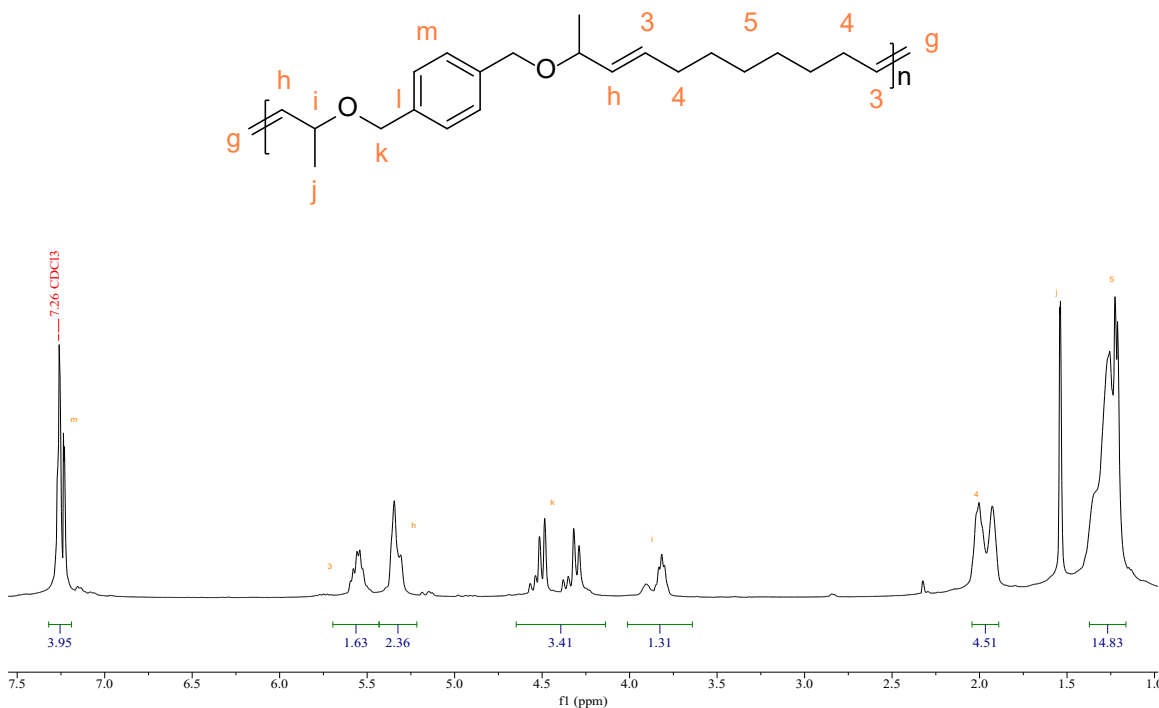


Figure 24. ^1H NMR spectrum of the copolymerization of M2 with G1 as the catalyst.

^1H NMR (400 MHz, Chloroform-*d*) δ 7.25 (aromatic, s, 4H), 5.55 (olefinic, h, $J = 9.3, 7.9$ Hz, 2H), 5.33 (olefinic, q, $J = 7.9, 7.0$ Hz, 2H), 4.65 – 4.14 (allylic, m, 4H), 4.01 – 3.64 (allylic, m, 2H), 2.04 – 1.89 (allylic, m, 4H), 1.37 – 1.16 (CH₂ and methyl, m, 14H).

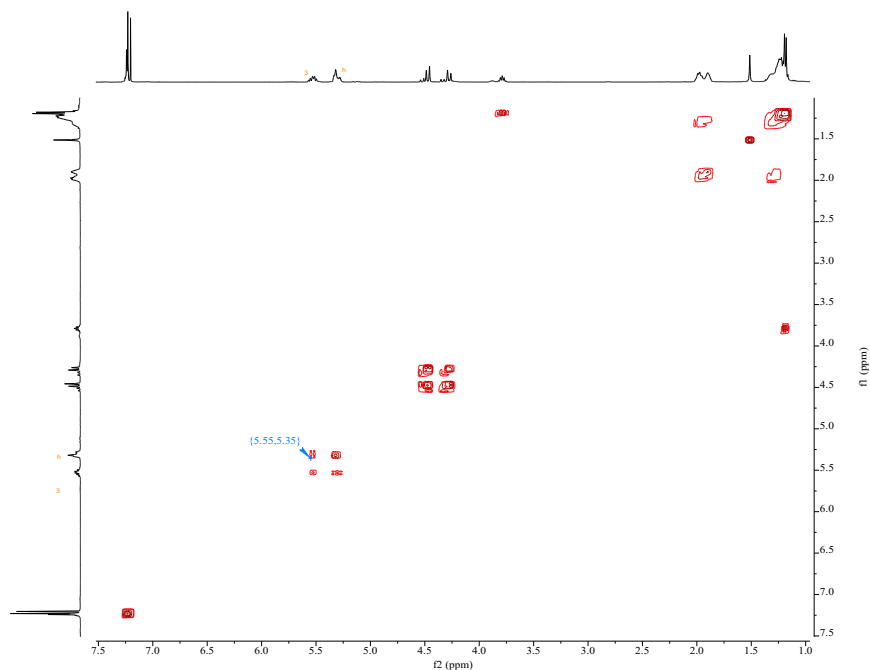


Figure 25. COSY NMR spectrum of the copolymerization of M2 with G1 as the catalyst.

4.3.2 Copolymerization of M3

M3 (242 mg, 0.88 mmol) was combined with 1,9-decadiene(148 mg, 1.07 mmol), **G1** (25 mg, 0.03 mmol), BQ (26 mg, 0.24 mmol), and BHT (48 mg, 0.22 mmol). After the 48 h reaction time at 60 °C, the reaction was cooled and quenched, and the polymer products were not precipitated and collected via rotavapor. The product is a black solid in yield of 0.370 g.

Similarly, for the second copolymerization attempt, **M3** (267 mg, 0.97 mmol) was combined with 1,9-decadiene(149 mg, 1.08 mmol), **G2** (20 mg, 0.03 mmol), BQ (25 mg, 0.23 mmol), and BHT (48 mg, 0.22 mmol). After the 48 h reaction time at 60 °C, the reaction was cooled and quenched, and the polymer products were precipitated and collected via filtration. The product is black solid in yield of 0.155 g.

The ^1H NMR spectrum of the product from the copolymerization of **M3** with **G1** is shown in Figure 26. The peaks r, q and p present same multiplicity as **M3**, and olefinic proton at 5.40 ppm could be the olefin on 1,9-decadiene homopolymer, which means copolymer was not formed.

The ^1H NMR spectrum of the precipitated material from the copolymerization of **M3** with **G2** is shown in Figure 27. It is different from the product of **M3** with **G1**, in which CH_2 groups (both 3.57 and 2.33) show double triplets, and methyl groups at 1.74 ppm are doublets. In COSY NMR, peak e and 7 have correlation, and it is the internal olefin between **M3** and 1,9-decadiene (Figure 28). GPC analysis was also carried out with the precipitated material from this reaction and the results indicated a polymer with $M_n=16200$ g/mol and $D=1.3$ for **M3** with **G1** and $M_n=3000$ g/mol and $D=1.3$ for **M3** with **G2**. Therefore, the product of **M3** with **G1** was homopolymer of 1,9-decadiene, and **M3** with **G2** formed copolymers under SADMET polymerization.

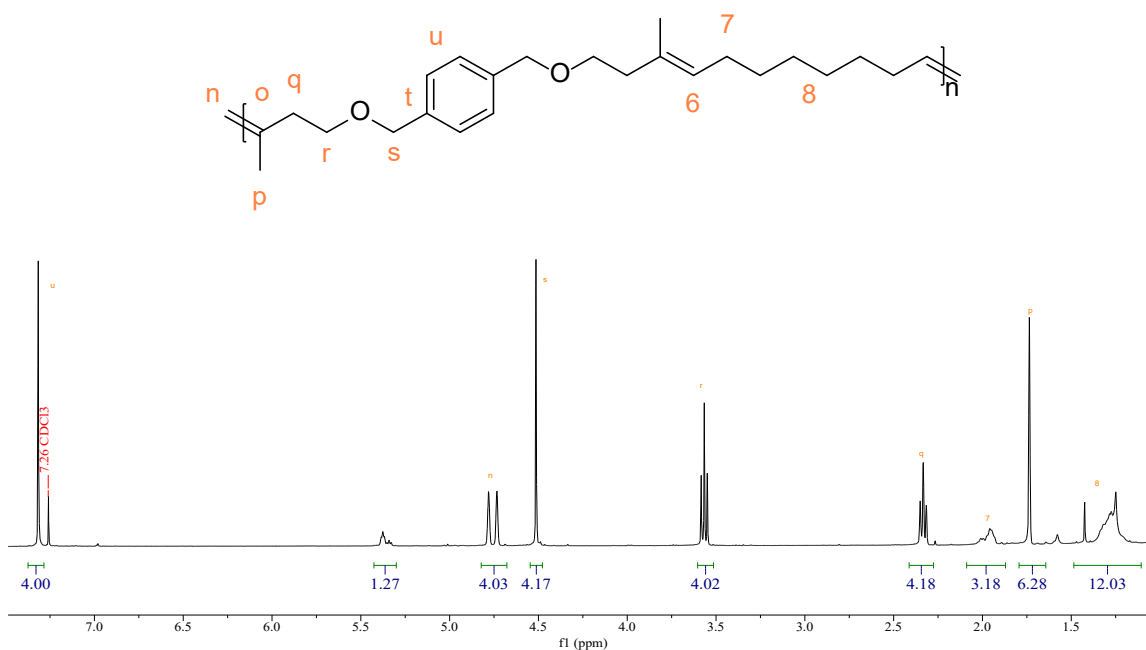


Figure 26. ^1H NMR spectrum of the copolymerization of **M3** with **G1** as the catalyst.

^1H NMR (400 MHz, Chloroform-*d*) δ 7.32 (aromatic, s, $J = 0.6$ Hz, 4H), 5.43 – 5.30 (m, 1H), 4.76 (olefinic, d, 4H), 4.51 (allylic, d, $J = 0.6$ Hz, 4H), 3.57 (CH_2 , t, $J = 6.9, 0.6$ Hz, 4H), 2.33 (CH_2 , t, 4H), 1.98 (allylic, d, $J = 22.2$ Hz, 3H), 1.74 (methyl, s, $J = 1.5, 0.8$ Hz, 6H), 1.49 – 1.11 (CH_2 , m, 12H).

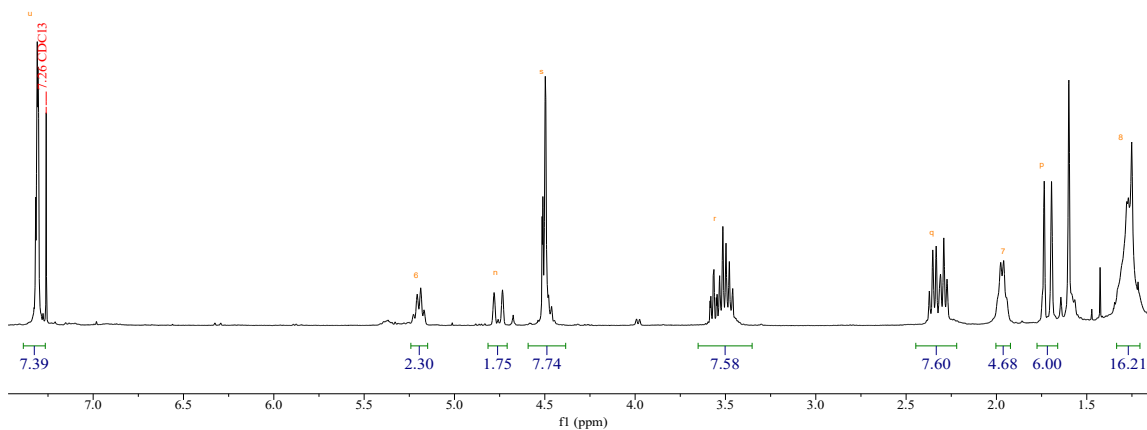


Figure 27. ^1H NMR spectrum of the copolymerization of M3 with G2 as the catalyst.

^1H NMR (400 MHz, Chloroform-*d*) δ 7.31 (aromatic, s, 8H), 5.20 (olefinic, q, $J = 8.0$ Hz, 2H), 4.74 (olefinic, d, 2H), 4.50 (allylic, s, 8H), 3.53 (CH_2 , td, 8H), 2.32 (CH_2 , dt, $J = 24.0, 7.4$ Hz, 8H), 1.97 (allylic, q, $J = 6.9$ Hz, 5H), 1.71 (methyl, d, 6H), 1.33 – 1.21 (CH_2 , m, 16H).

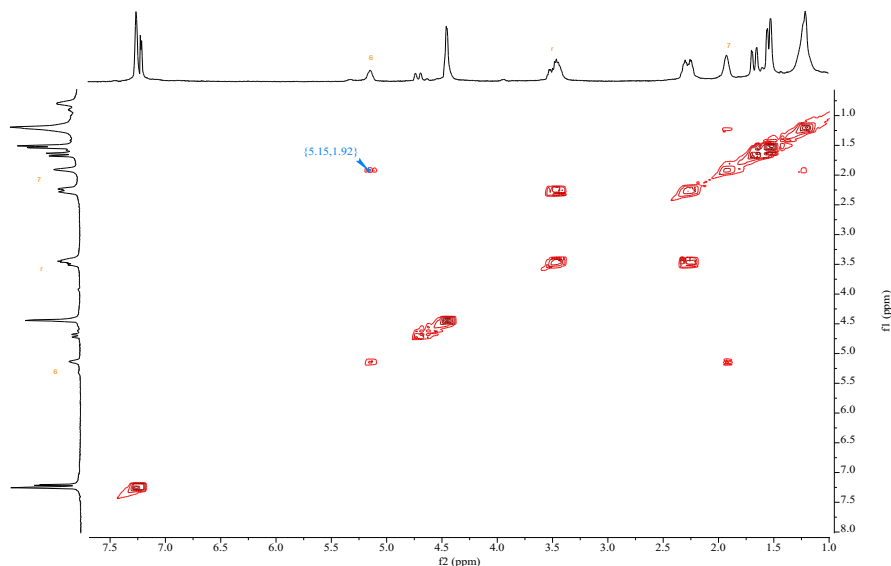


Figure 28. COSY NMR spectrum of the copolymerization of M3 with G2 as the catalyst.

4.3.3 Copolymerization of M4

M4 (240 mg, 0.89 mmol) was combined with 1,9-decadiene(143 mg, 1.03 mmol), **G1** (25 mg, 0.03 mmol), BQ (25 mg, 0.23 mmol), and BHT (45 mg, 0.20 mmol). After the 48-h reaction

time at 60 °C, the reaction was cooled and quenched, and the polymer products were not precipitated and collected via rotavapor. The product is a black solid in a yield of 0.259 g. Similarly, for the second copolymerization attempt, **M4** (238 mg, 0.87 mmol) was combined with 1,9-decadiene(134 mg, 0.97 mmol), **G2** (20 mg, 0.03 mmol), BQ (26 mg, 0.24 mmol), and BHT (50 mg, 0.23 mmol). After the 48-h reaction time at 60 °C, the reaction was cooled and quenched, and the polymer products were precipitated and collected via filtration. The product is a black solid in a yield of 0.202 g.

The ^1H NMR spectrum of the product from the homopolymerizations of **M4** with **G1** is shown in Figure 29, and the multiplicity is similar to **M4**, in which olefins present doublet doublet at 5.90 ppm and triplets at 5.17 ppm. The internal olefin on polyoctenamer is observed at 5.3ppm. The ^1H NMR spectrum of the precipitated material from the copolymerization of **M4** with **G2** is shown in Figure 30, and there are two kinds of olefin peaks (9 and w) at 5.50 ppm. In COSY NMR, peaks 9 and w show correlation to CH₂ groups on 1,9-decadiene at 2.00 ppm (Figure 31). GPC analysis was also carried out with the precipitated material from this reaction and the results indicated a polymer with $M_n=12600$ g/mol and $\bar{D}=1.7$ for **M4** with **G1** and $M_n=8300$ g/mol and $\bar{D}=1.4$ for **M4** with **G2**. We observed homopolymer of 1,9-decadiene by **G1**, and copolymer was formed with **G2**.

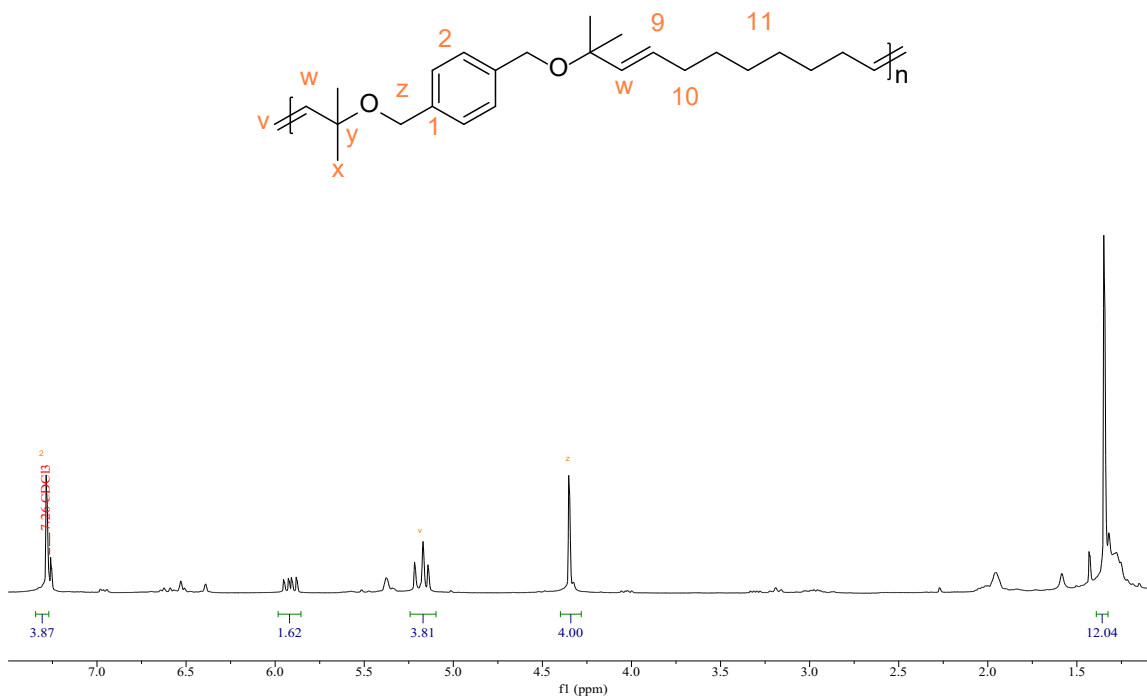


Figure 29. ^1H NMR spectrum of the copolymerization of M4 with G1 as the catalyst.

^1H NMR (400 MHz, Chloroform-*d*) δ 7.29 (aromatic, s, 4H), 5.98 – 5.85 (olefinic, ddp, 2H), 5.17 (olefinic, t, 4H), 4.34 (allylic, s, 4H), 1.34 (methyl, s, $J = 2.2$ Hz, 12H).

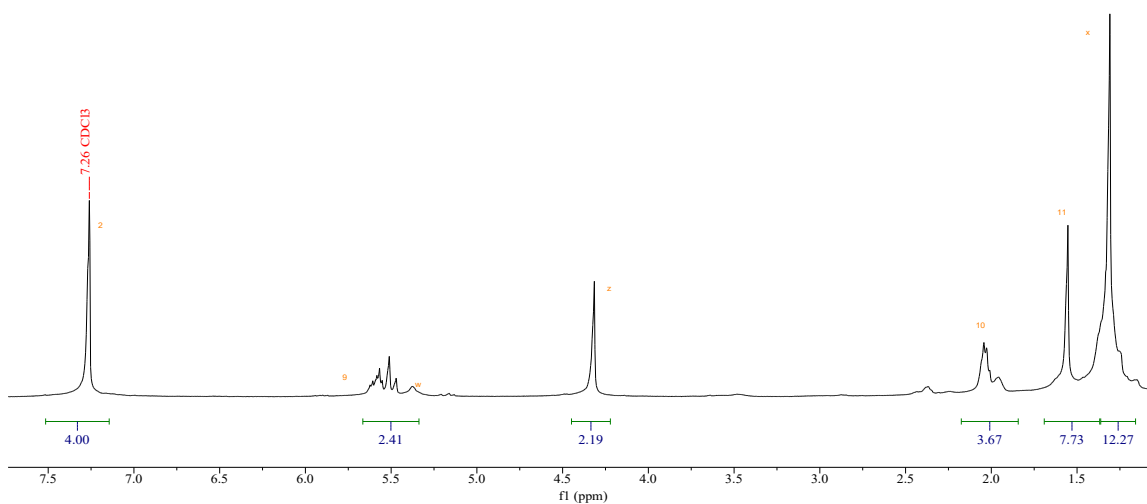


Figure 30. ^1H NMR spectrum of the copolymerization of M4 with G2 as the catalyst.

^1H NMR (400 MHz, Chloroform-*d*) δ 7.26 (aromatic, s, 4H), 5.67 – 5.34 (olefinic, m, 2H), 4.32 (allylic, s, 2H), 2.17 – 1.84 (CH_2 , m, 4H), 1.55 (CH_2 , s, 8H), 1.31 (methyl, s, 12H).

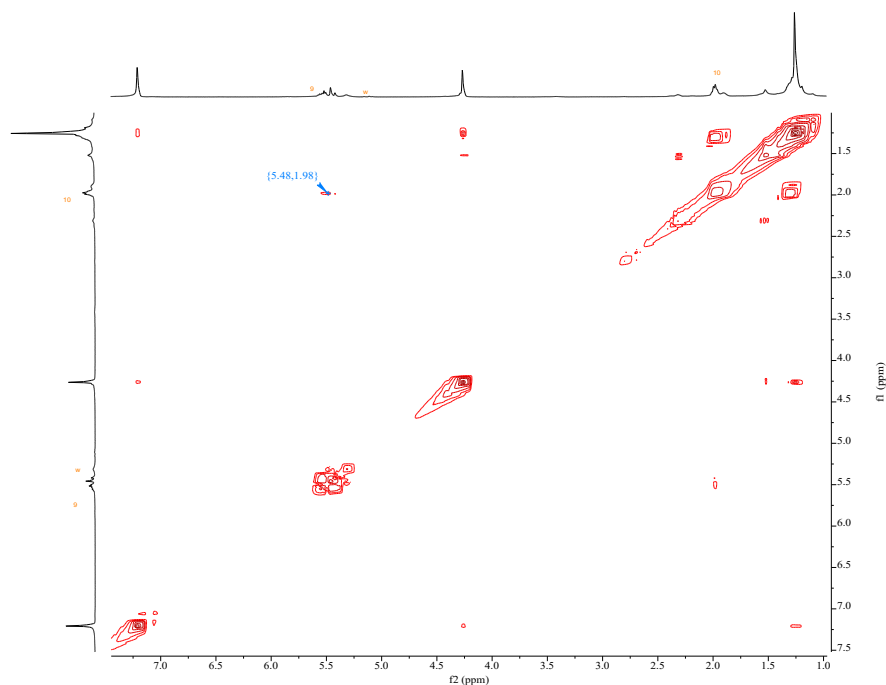


Figure 31. COSY NMR spectrum of the copolymerization of M4 with G2 as the catalyst.

4.4 Discussion

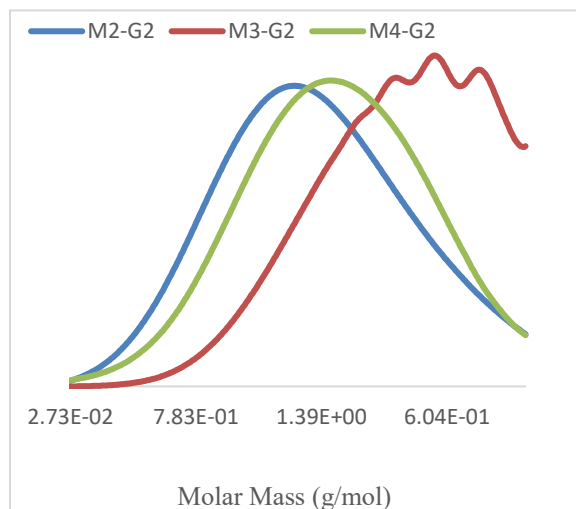


Figure 32. GPC analysis of copolymers.

M2, **M3**, and **M4** were copolymerized with 1,9-decadiene under SADMET conditions (1:1 moiety ratio) and GPC trace shows in Figure 32. In the reactions including 1,9-decadiene and **M2** with **G1**, **M3** with **G2**, and **M4** with **G2**, copolymers were formed and characterized by both

¹H and COSY NMR spectroscopy and GPC. Both Type II and III olefins are expected to selectively form alternating copolymer with Type I olefins to form alternating copolymers. **M2** with **G1**, **M3** with **G2**, and **M4** with **G2** presented desired properties, which classified as Type II or III olefins. **G2** increases **M4** reactivity by its own high activity in reactions. **M4** with **G2** formed polymer with higher molecular weight than **M3** with **G2**, and the molecular weight is similar to polymer form **M2** with **G1**, which is different from our expectations. The polymerizations of **M3** with **G1** and **M4** with **G1** were classified as Type IV by not deactivating catalysts and the formation of polyoctenamer.

Conclusion and Future Work

5.1 Conclusion

To explore more potential applications of ADMET polymerization, SADMET polymerization was set to react active (electron-rich and primary terminal) olefins with less active (electron-deficient or steric bulky) olefins in a 1:1 moiety ratio. Under SADMET conditions, alternating copolymers are formed by inserting less active olefin into the homopolymer of the active one. Both electronic and steric effects were observed. The electronic effect was brought by changing electron-rich α,ω -diene to electron-deficient one, and alternating copolymers were formed with diacrylamide in previous research.⁵⁸ The steric effects on olefin reactivity was shown in this project, and all polymerization results are included in the Table 4.

5.1.1 Olefin Categorization

In the research, ether was the functional group included in the backbone, which can tune polymer properties for more applications. Four benzyl ether olefins were structure confirmed with ¹H NMR spectrums and purified for further reactions. Designed olefins undergoes two polymerization processes to classify their reactivities: first, olefins were homopolymerized under ADMET conditions. Depending on the M_n of the product, the formation of homopolymer or oligomer were classified as Type I. Type II olefins may undergo CM under ADMET conditions, however, it difficultly observed CM in products. Secondly, olefins, not classified as Type I, were copolymerized with Type I olefin (1,9-decadiene in this research) under SADMET conditions. 1,9-decadiene were formed copolymer with Type II and III olefins. Type IV was not involved in polymerization and did not deactivate catalysts, which produced polyoctenamer. The olefin categorization helps rank olefin reactivity and predict whether alternating copolymer will be formed under SADMET polymerization conditions.

As results present below (Table 4), all olefins are classified into categorizations. **M1** shows same reactivity in both **G1** and **G2** as formations of homopolymers. Some synthetic efforts caused the M_n of homopolymer **M1** with **G2** is lower than **M1** with **G1**. It is necessary to repeat the entry and confirm results. Differently, **M2**, **M3**, and **M4** were classified into distinctive categorizations with **G1** and **G2**. **M2** with **G2** formed low M_n oligomers under ADMET conditions and classified as Type I. There was no polymer formed in the ADMET reactions of **M2** with **G1**, **M3**, and **M4** with **G1** and **G2**.

1,9-decadiene was used to further classify **M2**, **M3**, and **M4** under SADMET conditions. Since 1,9-decadiene is active and homopolymerize, the less active olefin, reacted and inserted in the chain of polyoctenamer, was from Type II or III. The copolymers were observed under SADMET conditions of **M2** with **G1**, **M3** with **G2** and **M4** with **G2**. Comparing the M_n of **M2** with **G1** and **M4** with **G2** polymers, **M2** with **G1** polymer contains more yield and higher M_n than **M4** with **G2**, and **M2** with **G1** is more active than **M4** with **G2**. Since the classifications of the olefins are gradient, **M2** with **G1** and **M4** with **G2** are identified as Type II/III olefins. **M2** with **G1** is a less Type II olefin, and **M4** is an active Type III olefin. **M3** with **G2** polymers have much lower yields and M_n than previous two olefins, and **M3** with **G2** is classified as less active Type III olefin. In the reaction of **M3** with **G1** and **M4** with **G1**, polyoctenamer proved that those two entries are Type IV, and the olefin did not deactivate catalyst.

5.1.2 Steric Effects

As hypothesized based on previous studies with cross metathesis, these novel ether olefins were observed to have decreased reactivity with increasing steric hindrance from **M1**<**M2**<**M4**<**M3** with **G1** and **G2** under ADMET polymerization conditions. **M1** was the most active olefin without any steric hindrance, and polymers with relatively high M_n homopolymer were formed with either **G1** or **G2**. **M2** has one methyl group on each side of alkyl adjacent to

ether and steric bulky, which was observed decreasing the reactivity with both catalysts than **M1** under the same conditions. The lower reactivity helps the formation of alternating copolymers with 1,9-decadiene. The decreasing reactivity is observed with **M4**, which includes two more methyl groups than **M2** at the same alkyl adjacent place. The addition of methyl groups make **M4** cannot be homopolymerized with **G2** and copolymerized with **G1**.

The structure design of **M3** twists the observations in either homopolymerization or copolymerization reactions in contract of **M2** and **M4**. In **M3**, two methyl groups are moved closer to the carbon double bonds, and steric environment is much crowder than **M2** and **M4**. As a result, **M3** did not participate in reactions with **G1** and formed low yield and M_n copolymers with **G2**. It is because that the methyl groups on vinyl carbon increases repulsive interaction of growing polymer and ligands on catalysts.⁵⁹

Table 4. Polymerization results and classifications of M1 – M4 with G1 and G2.

Entry	Monomer	Catalyst	Yield (g)	M_n (g/mol)	\bar{D}	Classification
1	M1	G1	0.404	5200	1.5	Type I
2	M1	G2	0.422	3800	1.7	Type I
3	M2	G2	0.383	1800	1.8	Type I
4	M2+1,9-decadiene	G1	0.285	8800	1.5	Type II
5	M3+1,9-decadiene	G1	N/A	N/A	N/A	Type IV
6	M3+1,9-decadiene	G2	0.155	3100	1.3	Type III
7	M4+1,9-decadiene	G1	N/A	N/A	N/A	Type IV
8	M4+1,9-decadiene	G2	0.202	8300	1.4	Type III

5.2 Future Works

After the **M1 – M4** were ranked reactivity and classified into categorizations, some analyses of polymers were not finished, such as polymer alternation, characterizations of **M1** under SADMET conditions, and analysis of reaction rate. The structure of **M1 – M4** contains a benzyl group placed between two ether groups, and it can be used to quantify the alternation of polymers. The alternation can be analyzed via liquid chromatography-mass spectrometry (LC-MS). After hydrogenating the polymer, the ether group will be cleaved and present either diol 1,9-decadiene or 1,9-decadiene oligomer. The alternation will help characterize the alternating copolymer. Also, to confirm the classification of **M1**, it is necessary to copolymerize **M1** with 1,9-decadiene for further studies. Although we did not characterize the polymerization rate, the studies of polymerization time and kinetics will improve olefin categorizations.

Future studies can explore more catalyst options for SADMET conditions to expand the research scope. In the research, all the polymerizations were catalyzed by **G1** or **G2**, and there are many variations of Grubbs catalysts, which may produce higher M_n polymers with lower catalyst loading and optimize the reaction conditions. In addition, the new catalysts used in SADMET conditions provide more possibility of finding new functional groups.

References

1. Grubbs, R. H.; Chang, S. Recent Advances in Olefin Metathesis and its Application in Organic Synthesis. *Tetrahedron*, **1998**, *54*, 4413–4450.
2. Astruc, D. The Metathesis Reactions: From a Historical Perspective to Recent Developments. *New. J. Chem.* **2005**, *29*, 42-56.
3. López, J. C.; Plumet, J. Metathesis Reactions of Carbohydrates: Recent Highlights in Cross-Metathesis. *Eur. J. Org. Chem.* **2011**, 1803–1825.
4. Anderson, A. W.; Merckling, N. G. Polymeric bicyclo-(2, 2, 1)-2-heptene. **1955**.
5. Casey, C. P. Development of the Olefin Metathesis Method in Organic Synthesis. *J. Chem. Educ.* **2006**, *83*, 192.
6. Grubbs, R. H. Olefin-Metathesis Catalysts for the Preparation of Molecules and Materials (Nobel Lecture). *Angew. Chem. Int. Ed.* **2006**, *29*, 42–56.
7. Vougioukalakis, G. C.; Grubbs, R. H. Ruthenium-Based Heterocyclic Carbene-Coordinated Olefin Metathesis Catalysts. *Chem. Rev.* **2010**, *110*, 1746–1787.
8. Choinopoulos, I. Grubbs' and Schrock's Catalysts, Ring Opening Metathesis Polymerization and Molecular Brushes—Synthesis, Characterization, Properties and Applications. *Polym. Chem.* **2019**, *11*, 298.
9. Dong, Y.; Matson, J. B.; Edgar, K. J. Olefin Cross-Metathesis in Polymer and Polysaccharide Chemistry: A Review. *Biomacromolecules*, **2017**, *18*, 1661–1676.
10. Schuster, M.; Blechert, S. Olefin Metathesis in Organic Chemistry. *Angew. Chem. Int. Ed.* **1997**, *36*, 2036–2056.
11. Chatterjee, A. K.; Sanders, D. P.; Grubbs, R. H. Synthesis of Symmetrical Trisubstituted Olefins by Cross Metathesis. *Org. Lett.* **2002**, *4*, 1939–1942.
12. Llevot, A.; Grau, E.; Carlotti, S.; Grelier, S.; Cramail, H. ADMET polymerization of bio-based biphenyl compounds. *Polym. Chem.* **2015**, *6*, 7693-7700.
13. Hassan, H. M. A. Recent applications of ring-closing metathesis in the synthesis of lactams and macrolactams. *Chem. Comm.* **2010**, *46*, 9100.
14. Monfette, S.; Fogg, D. E. Equilibrium Ring-Closing Metathesis. *Chem. Rev.* **2009**, *109*, 3783–3816.
15. Miller, S. J.; Blackwell, H. E.; Grubbs, R. H. Application of Ring-Closing Metathesis to the Synthesis of Rigidified Amino Acids and Peptides. *J. Am. Chem. Soc.* **1996**, *118*, 9606–9614.
16. Grubbs, R. H.; Miller, S. J.; Fu, G. C. Ring-Closing Metathesis and Related Processes in Organic Synthesis. *Acc. Chem. Res.* **1995**, *28*, 446–452.

17. Baughman, T. W.; Wagener, K. B. Recent Advances in ADMET Polymerization. *Springer Sci. Rev.* **2005**, 1–42.
18. Sutthasupa, S.; Shiotsuki, M.; Sanda, F. Recent Advances in Ring-Opening Metathesis Polymerization, and Application to Synthesis of Functional Materials. *Polym. J.* **2010**, *42*, 905–915.
19. Grubbs, R. H. Olefin Metathesis. *Tetrahedron*, **2004**, *60*, 7117–7140.
20. Hérisson, P. J.-L.; Chauvin, Y. Catalyse de Transformation Des Oléfines Par Les Complexes Du Tungstène. II. Télomérisation Des Oléfines Cycliques En Présence d'oléfines Acycliques. *Die Makromol. Chem.* **1971**, *141*, 161–176.
21. Chauvin, Y. Olefin Metathesis: The Early Days (Nobel Lecture). *Angew. Chem. Int. Ed.* **2006**, *45*, 3740–3747.
22. Pike, S. D.; Weller, A. S. Organometallic Synthesis, Reactivity and Catalysis in the Solid State Using Well-Defined Single-Site Species. *Phys. Eng. Sci.* **2015**, *373*, 20140187.
23. Trnka, T. M.; Grubbs, R. H. The Development of L₂X₂RuCHR Olefin Metathesis Catalysts: An Organometallic Success Story. *Acc. Chem. Res.* **2001**, *34*, 18–29.
24. Grela, K.; Harutyunyan, S.; Michrowska, A. A Highly Efficient Ruthenium Catalyst for Metathesis Reactions. *Angew. Chem. Int. Ed.* **2002**, *41*, 4038–4040.
25. Ogba, O. M.; Warner, N. C.; O'Leary, D. J.; Grubbs, R. H. Recent Advances in Ruthenium-Based Olefin Metathesis. *Chem. Soc. Rev.* **2018**, *47*, 4510–4544.
26. Dias, E. L.; Nguyen, S. T.; Grubbs, R. H. Well-Defined Ruthenium Olefin Metathesis Catalysts: Mechanism and Activity. *J. Am. Chem. Soc.* **1997**, *119*, 3887–3897.
27. Murdzek, J. S.; Schrock, R. R. Well-Characterized Olefin Metathesis Catalysts that Contain Molybdenum. *Organometallics.* **1987**, *6*, 1373–1374.
28. Schrock, R. R. Multiple Metal–Carbon Bonds for Catalytic Metathesis Reactions. *Angew. Chem. Int. Ed.* **2006**, *45*, 3748–3759.
29. Caire Da Silva, L.; Rojas, G.; Schulz, M. D.; Wagener, K. B. Acyclic Diene Metathesis Polymerization: History, Methods and Applications. *Prog. Polym. Sci.* **2017**, *69*, 79–107.
30. Nguyen, S. T.; Grubbs, R. H.; Ziller, J. W. Syntheses and Activities of New Single-Component, Ruthenium-Based Olefin Metathesis Catalysts. *J. Am. Chem. Soc.* **1993**, *115*, 9858–9859.
31. Atallah, P.; Wagener, K. B.; Schulz, M. D. ADMET: The Future Revealed. *Macromolecules.* **2013**, *46*, 4735–4741.

32. Sauty, N. F.; Da Silva, L. C.; Schulz, M. D.; Few, C. S.; Wagener, K. B. Acyclic Diene Metathesis Polymerization and Precision Polymers. *Appl. Petrochem. Res.* **2014**, *4*, 225–233.
33. Opper, K. L.; Wagener, K. B. ADMET: Metathesis Polycondensation. *J. Polym. Sci.* **2011**, *49*, 821–831.
34. Ding, L.; Yang, G.; Xie, M.; Gao, D.; Yu, J.; Zhang, Y. More Insight into Tandem ROMP and ADMET Polymerization for Yielding Reactive Long-Chain Highly Branched Polymers and their Transformation to Functional Polymer Nanoparticles. *Polymer*. **2012**, *53*, 333–341.
35. Pribyl, J.; Wagener, K. B.; Rojas, G. ADMET Polymers: Synthesis, Structure Elucidation, and Function. *Mater. Chem. Front.* **2021**, *5*, 14–43.
36. Wagener, K. B.; Boncella, J. M.; Nel, J. G. Acyclic Diene Metathesis (ADMET) Polymerization. *Macromolecules*. **1991**, *24*, 2649–2657.
37. Schulz, M. D.; Wagener, K. B. Precision Polymers through ADMET Polymerization. *Macromol. Chem. Phys.* **2014**, *215*, 1936–1945.
38. Sworen, J. C.; Smith, J. A.; Wagener, K. B.; Baugh, L. S.; Rucker, S. P. Modeling Random Methyl Branching in Ethylene/ Propylene Copolymers Using Metathesis Chemistry: Synthesis and Thermal Behavior. *J. Am. Chem. Soc.* **2003**, *125*, 2228–2240.
39. Winkler, M.; Mueller, J. O.; Oehlenschlaeger, K. K.; Montero De Espinosa, L.; Meier, M. A. R.; Barner-Kowollik, C. Highly Orthogonal Functionalization of ADMET Polymers via Photo-Induced Diels–Alder Reactions. *Macromolecules*. **2012**, *45*, 5012–5019.
40. Li, H.; Caire Da Silva, L.; Schulz, M. D.; Rojas, G.; Wagener, K. B. A Review of how to do an Acyclic Diene Metathesis Reaction. *Polym. Int.* **2017**, *66*, 7–12.
41. Song, S.; Miao, W.; Wang, Z.; Gong, D.; Chen, Z.-R. Synthesis and Characterization of Precisely-Defined Ethylene-o-aryl Ether Polymers via ADMET Polymerization. *Polymer*. **2015**, *64*, 76–83.
42. Schulz, M. D.; Wagener, K. B. Solvent Effects in Alternating ADMET Polymerization. *ACS. Macro. Letters*. **2012**, *1*, 449–451.
43. Silvaa, L. C.; Rojasb, G.; Schulzc, M.; Wagener, K. B. Acyclicdienemetathesispolymerization:History, Methodsandapplicatio. *Prog. Polym. Sci.* **2016**, *69*, 79–107.
44. Li, Z.; Li, L.; Deng, X.; Lv, A.; Wang, Z.; Du, F.; Li, Z. Ethylene–Ethyl Acrylate Copolymers via ADMET Polymerization: Effect of Sequence Distribution on Thermal Properties. *Polym. Chem.* **2013**, *51*, 2900–2909.
45. Gorodetskaya, I. A.; Choi, T.-L.; Grubbs, R. H. Hyperbranched Macromolecules via Olefin Metathesis. *J. Am. Chem. Soc.* **2007**, *129*, 12672–12673.

46. Lucero, J. M.; Romero, Z.; Moreno, A.; Huber, D. L.; Simock, C. ADMET Polymerization in Affordable, Commercially Available, High Boiling Solvent. *SN Appl. Sci.* **2020**, *2*, 647.
47. Fokou, P. A.; Meier, M. A. R. Studying and Suppressing Olefin Isomerization Side Reactions During ADMET Polymerizations. *Macromol. Rapid Commun.* **2010**, *31*, 368–373.
48. Choi, T.; Rutenberg, I. M.; Grubbs, R. H. Synthesis of A,B-Alternating Copolymers by Ring-Opening-Insertion-Metathesis Polymerization.pdf. *Angew. Chem. Int. Ed.* **2002**, *41*.
49. Demel, S.; Slugovc, C.; Stelzer, F.; Fodor-Csorba, K.; Galli, G. Alternating Diene Metathesis Polycondensation (ALTMET) – A Versatile Tool for the Preparation of Perfectly Alternating AB Copolymers.pdf. *Macromol. Rapid Commun.* **2003**, *24*, 636–641.
50. Chatterjee, A. K.; Choi, T.; Sanders, D. P.; Grubbs, R. H. A General Model for Selectivity in Olefin Cross Metath. *J. AM. CHEM. SOC.* **2003**, *125*, 11360–11370.
51. Lucero, J. M.; Romero, Z.; Moreno, A.; Huber, D. L.; Simocko, C. ADMET Polymerization in Affordable, Commercially Available, High Boiling Solvent. *SN Appl. Sci.* **2020**, *2*, 647.
52. Barbaraa, I.; Flourata, A. L.; Al, F. Renewable Polymers Derived from Ferulic Acid and Biobaseddiols via ADME. *Eur. Polym. J.* **2015**, *62*, 236–243.
53. Vlaminck, L.; Lingier, S.; Hufendiek, A.; Prez, F. Lignin Inspired Phenolic Polyethers Synthesized via ADMET: Systematic Structure-Property. *Eur. Polym. J.* **2017**, *95*, 503–513.
54. Hong, S. H.; Sanders, D. P.; Lee, C. W.; Grubbs, R. H. Prevention of Undesirable Isomerization during Olefin Metathesis. *J. Am. Chem. Soc.* **2005**, *127*, 17160–17161.
55. Meng, X.; Matson, J. B.; Edgar, K. J. Olefin Cross-Metathesis, a Mild, Modular Approach to Functionalized Cellulose Esters. *Polym. Chem.* **2014**, *5*, 7021–7033.
56. Silverstein, R. M.; Webster, F. X.; Kiemle, D. J.; Bryce, D. L. *Spectrometric Identification of Organic Compounds*; Wiley: New Jersey, 2015.
57. Nishimori, K.; Ouchi, M. AB-Alternating Copolymers via Chain-Growth Polymerization: Synthesis, Characterization, Self-Assembly, and Functions. *Chem. Comm.* **2020**, *56*, 3473–3483.
58. Konzelman, J. Ph.D. Dissertation, University of Florida, 1993.
59. Martinez, H.; Miró, P.; Charbonneau, P.; Hillmyer, M. A.; Cramer, C. J. Selectivity in Ring-Opening Metathesis Polymerization of Z-Cyclooctenes Catalyzed by a Second-Generation Grubbs Catalyst. *ACS Catal.* **2012**, *2*, 2547–2556.